



BRNO UNIVERSITY OF TECHNOLOGY

VYSOKÉ UČENÍ TECHNICKÉ V BRNĚ

FACULTY OF MECHANICAL ENGINEERING

FAKULTA STROJNÍHO INŽENÝRSTVÍ

INSTITUTE OF SOLID MECHANICS, MECHATRONICS AND BIOMECHANICS

ÚSTAV MECHANIKY TĚLES, MECHATRONIKY A BIOMECHANIKY

POSSIBILITIES OF THE DESCRIPTION OF STRESS– STRAIN CURVES FOR COMPUTATIONAL SIMULA- TIONS

MOŽNOSTI POPISU KŘIVEK NAPĚTÍ–PŘETVOŘENÍ PRO VÝPOČTOVÉ SIMULACE

BACHELOR'S THESIS

BAKALÁŘSKÁ PRÁCE

AUTHOR

AUTOR PRÁCE

Josef Košťál

SUPERVISOR

VEDOUCÍ PRÁCE

Ing. František Šebek, Ph.D.

BRNO 2018

Bachelor's Thesis Assignment

Institut: Institute of Solid Mechanics, Mechatronics and Biomechanics
Student: **Josef Košťál**
Degree program: Engineering
Branch: Fundamentals of Mechanical Engineering
Supervisor: **Ing. František Šebek, Ph.D.**
Academic year: 2017/18

As provided for by the Act No. 111/98 Coll. on higher education institutions and the BUT Study and Examination Regulations, the director of the Institute hereby assigns the following topic of Bachelor's Thesis:

Possibilities of the description of stress-strain curves for computational simulations

Brief description:

Carry out the research study on the possible relationships for description of stress-strain curves used for computational simulations in the conditions of severe plastic deformations. Find the piece-wise linear stress strain relationship for a given output of the tensile test of 18CrNiMo7-6 structural steel using the finite element method on the basis of comparison of force responses from simulation and experiment. Then, apply the chosen approximation relationships to the found curve and formulate the conclusions about their usability.

Bachelor's Thesis goals:

1. Research study on the possible relationships describing the stress-strain curve.
2. Obtaining the piece-wise linear stress-strain relationship for a given steel using the finite element method.
3. Creating the user interface for obtaining the material constants of chosen approximation relationships.
4. Application of chosen approximation relationships and formulation of conclusions about their usability.

Recommended bibliography:

LUDWIK, P.: Elemente der Technologischen Mechanik. Julius Springer, Berlin, 1909

HOLLOMON, J. H.: Tensile deformation. Metals Technology, pp. 268-290, 1945

SWIFT, H. W.: Plastic instability under plane stress. Journal of the Mechanics and Physics of Solids, vol. 1, no. 1, pp. 1-18, DOI:10.1016/0022-5096(52)90002-1, 1952

KLEEMOLA, H. J., NIEMINEN, M. A.: On the strain-hardening parameters of metals. Metallurgical Transactions, vol. 5, no. 8, pp. 1863-1866, DOI:10.1007/BF02644152, 1974

KOC, P., ŠTOK, B.: Computer-aided identification of the yield curve of a sheet metal after onset of necking. Computational Materials Science, vol. 31, no. 1-2, pp. 155-168, DOI:10.1016/j.commatsci.2004.02.004, 2004

MIRONE, G.: A new model for the elastoplastic characterization and the stress-strain determination on the necking section of a tensile specimen. International Journal of Solids and Structures, vol. 41, no. 13, pp. 3545-3564, DOI:10.1016/j.ijsolstr.2004.02.011, 2004

JOUN, M., EOM, J. G., LEE, M. Ch.: A new method for acquiring true stress-strain curves over a large range of strains using a tensile test and finite element method. Mechanics of Materials, vol. 40, no. 7, pp. 586-593, DOI:10.1016/j.mechmat.2007.11.006, 2008

KAMAYA, M., KAWAKUBO, M.: A procedure for determining the true stress-strain curve over a large range of strains using digital image correlation and finite element analysis. Mechanics of Materials, vol. 43, no. 5, pp. 243-253, DOI:10.1016/j.mechmat.2011.02.007, 2011

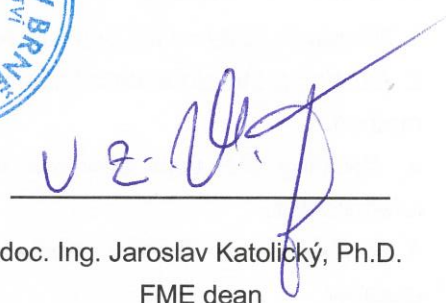
JENÍK, I., KUBÍK, P., ŠEBEK, F., HŮLKA, J., PETRUŠKA, J.: Sequential simulation and neural network in the stress-strain curve identification over the large strains using tensile test. Archive of Applied Mechanics, vol. 87, no. 6, pp. 1077-1093, DOI:10.1007/s00419-017-1234-0, 2017

Students are required to submit the thesis within the deadlines stated in the schedule of the academic year 2017/18.

In Brno, 29. 9. 2017



prof. Ing. Jindřich Petruška, CSc.
Director of the Institute



doc. Ing. Jaroslav Katolický, Ph.D.
FME dean

Abstract

This bachelor's thesis investigated the identification of material's flow curve using experimental data from standard tensile test output, and the possibilities of fitting a non-linear relationship through this identified curve. The theoretical background of differences between engineering and true stress and strain was presented, as well as the tensile test basis and its output. An analytical correction method (Mirone-La Rosa) for flow curve's trend estimation, using the tensile test as an input, was described and used. Elasto-plastic piece-wise linear material models were listed and additionally four non-linear relationships were chosen and investigated – Hollomon, Ludwik, Swift and Voce. Then, the finite element method was used for flow curve identification of experimentally tested 18CrNiMo7-6 steel, with a standard tensile test output needed for flow curve calibration. Flow curve was calibrated with iterative process on the basis of comparison of reaction forces from simulation and experiment. Furthermore, the user interface was created, and the best fit out of four chosen non-linear relationships was found.

Keywords

flow curve, finite element method, plasticity, MLR correction, tensile test, data regression, non-linear material model

Rozšířený abstrakt

Tato bakalářská práce se zabývá problematikou určování křivky napětí–přetvoření z experimentálně změřených dat tahové zkoušky a regresí této zjištěné křivky nelineárními vztahy.

V úvodní kapitole jsou nadefinovány cíle a motivace této práce. V konvenčním strojírenství se obvykle pohybujeme v napětích do hodnoty meze kluzu, protože se snažíme eliminovat vznik plastické deformace, a tedy křivka napětí–přetvoření je po dosažení hodnoty meze kluzu nezajímavá. Existují však specifické aplikace, které využívají rozsáhlé plastické deformace pro změnu tvaru materiálu – např. tvářecí procesy. Abychom byli schopni tyto procesy numericky simulovat, je potřeba znát křivku zpevnění i po vytvoření krčku v rozsáhlých plastických deformacích. Materiálový model je kritickým vstupem do numerické simulace, a bez jeho věrohodné reprezentace není možné získat reálné výsledky. Práce se dále zabývá možnostmi popsání získané křivky zpevnění nelineárními vztahy, které nám dovolují vyšetřovat vlastnosti materiálu pomocí různých materiálových konstant, přičemž některé z nich mají technologický význam.

V druhé kapitole je pak dán teoretický základ o tahové zkoušce a jejím výstupu. Jsou popsány rozdíly mezi smluvním a skutečným napětím a smluvním a skutečným přetvořením. Jsou popsány význačné body na křivce, jako mez kluzu, mez pevnosti, mez úměrnosti, smluvní mez kluzu, atd. Dále jsou popsány analytické vztahy smluvních a skutečných napětí a přetvoření a

jsou vymezeny jejich intervaly platnosti. Pozornost je věnována pouze tvárným materiálům bez výrazné meze kluzu, protože popsání deformace při výrazné mezi kluzu v následujících kapitolách by bylo nad rámec bakalářské práce. Je zde zmíněna analytická korekce Mirone-La Rosa (MLR), pomocí které je možné odhadnout trend křivky zpevnění (taktéž „*flow curve*“) ve skutečných souřadnicích po vytvoření krčku. Touto metodou získáváme odhad trendu redukovaného průměrného napětí jako funkci redukovaného průměrného přetvoření.

Třetí kapitola se zabývá elasto-plastickými materiálovými modely. Popisuje matematické možnosti popisu křivek zpevnění pro výpočtové simulace – ideální elasto-plastický model, bilineární a multilineární. Dále byly vybrány 4 nelineární možnosti popisu křivek – Hollomon, Ludwik, Swift a Voce. Každý z těchto vztahů je detailněji rozebrán a jsou popsány jejich jednotlivé parametry.

Zmíněné kapitoly dávají teoretický základ, který je následně aplikován na ocel 18CrNiMo7-6, která byla změřena zkouškou tahem na Ústavu materiálových věd a inženýrství a jejíž výstup byl poskytnut vedoucím.

Ve čtvrté kapitole je rozebrána problematika numerického určení křivky zpevnění. Iterační výpočtová metoda je použita v této práci. Tahová zkouška byla numericky simulována metodou konečných prvků v programu ANSYS Mechanical APDL 18.1, přičemž byl celý problém zpracován jako makro v parametrickém jazyce APDL. Tímto byla zaručena maximální parametrizovatelnost. Numerické určení křivky zpevnění spočívá v ladění materiálového vstupu na základě silové odezvy ze simulace, která je porovnána s experimentální. Autor provedl 26 iterací pro nalezení optimální křivky zpevnění. Ta byla zkalibrována s experimentem tak, že rozdíly v silové odezvě jsou méně než 1,5 % v oblasti plastické nestability. Makro je přiloženo v příloze, současně se skriptem vytvořeném v programu MATLAB, sloužícím pro porovnání silové odezvy experimentu a simulace. Dále je přiložena tabulka s procentuálními rozdíly experimentu a simulace.

Pátá kapitola potom aplikuje nelineární vztahy z kapitoly třetí. Bylo vytvořeno uživatelské prostředí v programu MATLAB verze R2016a, které slouží k nalezení optimální regrese zjištěné křivky zpevnění. Tento nástroj hledá minimum chyby ve smyslu nejmenších čtverců, přičemž zobrazí optimální nalezenou křivku v závislosti na vstupních odhadech parametrů. Odhady vstupních parametrů jsou při regresi nelineárními vztahy kritickým místem, protože řešení metody nejmenších čtverců může konvergovat pouze k nalezení lokálního minima problému, avšak ne globálního. Vstupy do vytvořeného uživatelského prostředí jsou zde popsány společně s jeho návodem k použití. Vytvořené uživatelské prostředí je taktéž přiloženo jako příloha v elektronické podobě.

Dále jsou rozebrány výsledky regrese. Jako nejlepší nelineární vztah pro danou ocel byl nalezen Swift s nejmenší hodnotou chyby vzniklé při regresi ve smyslu nejmenších čtverců. Dále byly porovnány vlastnosti materiálových konstant, nalezených vytvořeným nástrojem. Bylo zjištěno, že hodnota exponentu u vztahu „Hollomon“ n_H neodpovídá vypočtené hodnotě skutečného přetvoření na mezi pevnosti ε_u – procentuální rozdíl byl vypočten 64,2 %. Zjištěné parametry tohoto vztahu – koeficient deformačního zpevnění a exponent deformačního zpevnění – by se daly využít v technologických aplikacích např. při tvářecích operacích pro určení hodnoty skutečného napětí potřebného pro určitou hodnotu skutečného přetvoření. Také byla nalezena dobrá korelace parametru A_V ze vztahu „Voce“ s hodnotou smluvního napětí $s_{p0,1}$. Tento parametr vyjadřuje počáteční napětí, při němž začne být znatelná homogenní plastická deformace. Procentuální rozdíl těchto dvou hodnot byl vypočten 0,7 %.

Závěrem jsou potom shrnuty získané poznatky a výsledky. Práce by mohla být nadále rozvinuta optimalizací a automatizací procedury určování *flow curve*. Je obtížné vyvinout univerzální

automatickou metodu, poněvadž vlastnosti materiálů se významně liší v různých odvětvích strojího inženýrství. Zvláště obtížný je popis výrazné meze kluzu – tzv. Lüdersovy deformace. Byly navrženy nové metody (sekvenční simulace, soft computing – neuronové sítě), avšak jejich všestranné použití je omezené a mohly by být dále zkoumány a optimalizovány.

Klíčová slova

křivka tečení, metoda konečných prvků, plasticita, MLR korekce, zkouška tahem, regrese dat, nelineární materiálový model

KOŠTÁL, J. *Possibilities of the description of stress–strain curves for computational simulations*. Brno: Brno University of Technology, Faculty of Mechanical Engineering, 2018. 45 p. Supervisor Ing. František Šebek, Ph.D..

I declare that I have written the bachelor's thesis *Possibilities of the description of stress–strain curves for computational simulations* on my own, under the supervision of my supervisor Ing. František Šebek, Ph.D., using the sources listed in references.

May 17, 2018

Josef Košťál



I wish to express my sincere gratitude to my supervisor Ing. František Šebek, Ph.D. for his great and empathic attitude and dedication to share knowledge.

Contents

1. Introduction.....	13
2. Types of stress–strain curves	14
2.1. Tensile test.....	14
2.2. Engineering stress–strain curve.....	15
2.3. Additional tensile test outputs	17
2.4. True stress–true strain curve	18
2.5. MLR Correction	19
3. Non-linear stress–strain relationships	21
3.1. Constitutive elasto-plastic material model	21
3.2. Hollomon.....	22
3.3. Ludwik	24
3.4. Swift	25
3.5. Voce	26
4. Identification of flow curve using the finite element method.....	28
4.1. Introduction	28
4.2. Stress–strain curves	28
4.3. Flow curve calibration and tensile test finite element simulation.....	29
4.3.1. APDL Macro	31
4.3.2. Results	33
5. Application of chosen non-linear relationships	36
5.1. The user interface	36
5.2. Results of fitting	38
6. Summary and conclusion.....	41
7. References.....	42
8. Lists.....	43
8.1. List of abbreviations.....	43
8.2. List of variables.....	43
8.3. List of attachments	45

1. Introduction

In conventional mechanical engineering, the occurrence of plastic deformation is generally being eliminated, and therefore, the region of the stress–strain curve beyond the yield point is being disregarded. However, as some specific applications are using plastic deformations to change the shape of materials (e.g. forming processes), some are interested in the region of the stress–strain curve beyond the yield point value. The material model input plays key role to obtain reliable results in computational simulations. This thesis is centred around the following research questions and tasks:

- How can the conventional output of tensile testing be applied in order to gain values of a true stress–true strain? The tensile test is the most widely used fundamental mechanical test for gaining material data. Its standard output is the force–elongation curve. This output is usually recalculated into the engineering stress–strain curve, but it is possible to derive the true stress–true strain curve by using certain methods.
- A research study of possible descriptions of true stress–true strain curves. This is a frequently used approach, which describes the plastic region of a curve with additional parameters and material constants. Four non-linear relationships were chosen and investigated.
- Identification of the piece-wise linear true stress–true strain curve (the so-called flow curve) from the measured steel 18CrNiMo7-6. Only standard force–elongation tensile test output is needed for the finite element method (FEM) simulation. The flow curve is calibrated using an iterative process.
- Development of an interface, which applies the previously-mentioned relationships on an identified flow curve of given steel.
- Comparison of the true stress–true strain curve calibrated using FEM simulation and its regression by four chosen non-linear relationships. Conclusions of their usability and fit.

2. Types of stress–strain curves

2.1. Tensile test

The tensile test is the most fundamental, widely-used and standardised material test. During the tensile test, the specimen is loaded uniaxially by displacement along its length and 2 quantities are simultaneously measured – the applied load F , typically measured by the load cell, and elongation L , measured by the extensometer. The reason why the elongation is not measured from the crosshead displacement is because otherwise the results would be influenced by machine stiffness, which is undesirable [1].

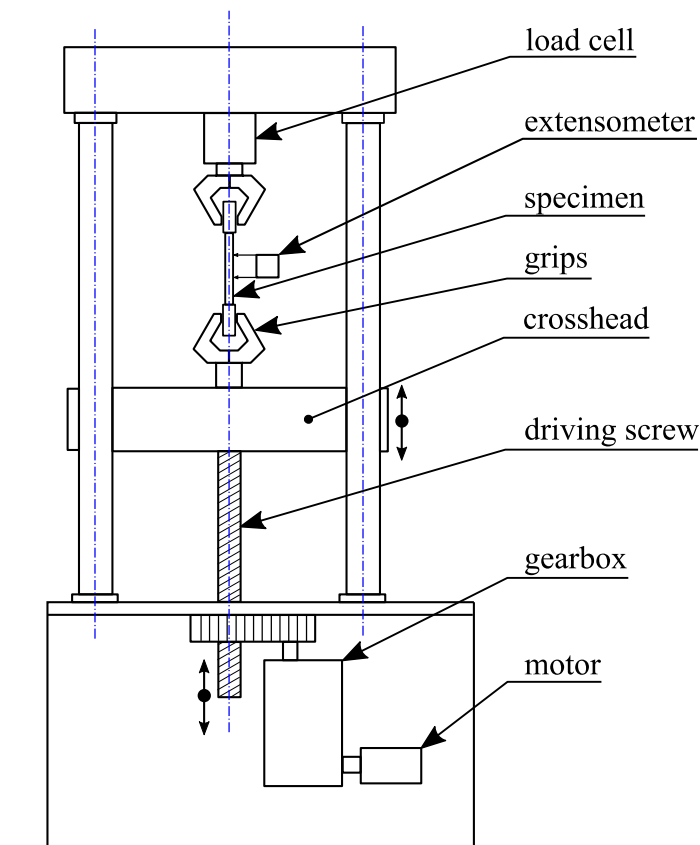


Figure 1 Schema of the universal electromechanical testing machine. Modified from [1]

Apart from electromechanical testing machines, servo hydraulic machines can also be used. A hydraulic testing machine can supply forces of greater magnitude (more than 4450 kN) more economically as compared to the screw driven machine. That is because the production cost of the driving screw rises together with the nominal force [1].

The definition of the recommended geometry of specimens is standardised, generally with the circular or rectangular cross section. The specification of the geometry is described in Czech and European standard ČSN EN 10002-1. In the United States, the geometry is further specified in American Standard for Testing and Materials ASTM E8 [1]. Besides geometry, more factors

have an influence on the results – the speed of deformation, the surrounding temperature and prior history of plastic deformation [1]. Testing is usually done quasi-statically, however in some cases – for example investigation of material properties for specific forming processes – the speed of deformation (together with the temperature) has a decisive effect on results. The tensile test is then done with increased temperature and strain rate. To be able to describe such processes, the viscous part of behaviour (dependence of material hardening on strain rate, creep and stress relaxation) needs to be taken into account. Therefore, the visco-plastic material model is being used in such cases [2]. Since this thesis is aimed on the standard tensile test output, this approach will not be further investigated, and only the elasto-plastic model will be investigated.

2.2. Engineering stress–strain curve

The output from the tensile test is the load–elongation dependency. This data is then recalculated into a conventionally-used engineering stress–strain curve. The engineering stress s is computed by dividing the applied load F by the original cross-sectional area of the specimen A_0

$$s = \frac{F}{A_0} \quad (1)$$

The engineering strain e is defined as

$$e = \frac{L - L_0}{L_0} = \frac{\Delta L}{L_0} \quad (2)$$

where L is instantaneous deformed length, ΔL is elongation increment and L_0 is the original undeformed length of the specimen, the so-called gauge length [1]. If the test was realised in the presence of an extensometer, the L_0 is substituted with L_{0ext} , which is the distance between the extensometer's clips. A typical engineering stress–strain curve is depicted in Figure 2.

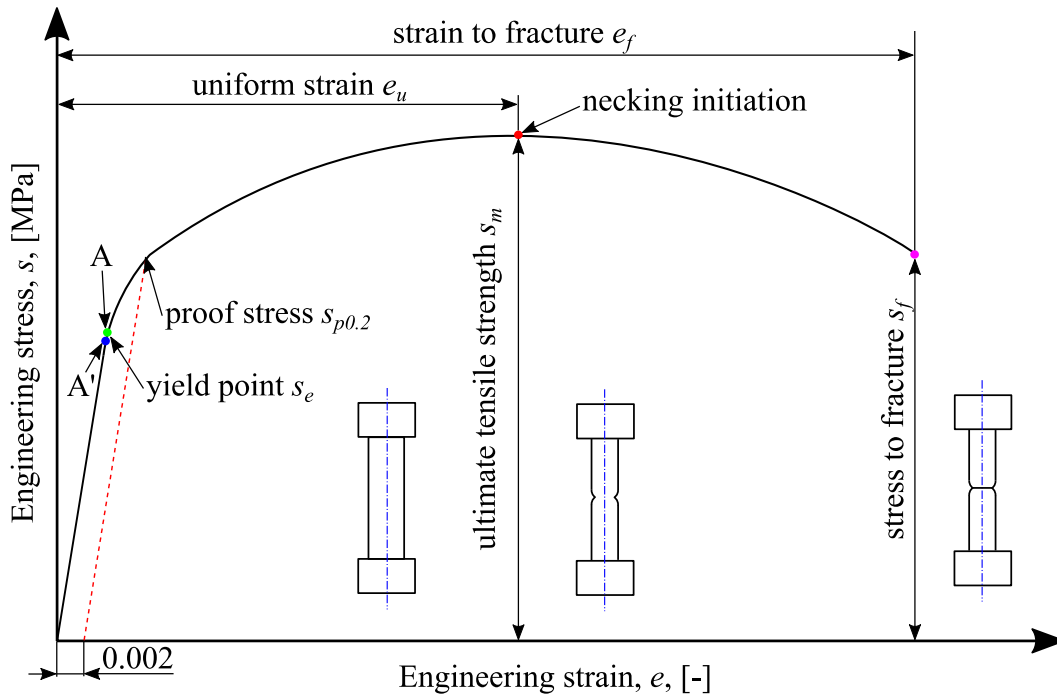


Figure 2 Typical stress–strain curve of ductile steel. Modified from [1]

Point A' is the proportional limit. Until this point, the relationship between stress and strain is proportional and described by Hooke's law (see equation (4)). The elastic limit – point A – succeeds the proportional limit and is defined as the greatest stress the material is able to withstand without any measurable residual permanent strain; after the complete unload of the specimen [1].

The yield point is the point where the first plastic deformation occurs. The location of this point depends on the material properties and behaviour. According to Figure 2, the yield point would be the point where the curve deflects from its linear part. But, an experimentally determined yield point in this manner would be dependent on extensometer sampling sensitivity. Therefore, the offset yield stress value is introduced: the so-called proof stress. It is a covenanted value of stress magnitude creating certain plastic deformation. Conventionally, the proof stress $s_{p0.2}$ which gives the plastic deformation of $e = 0.002$ ($= 0.2\%$) is used. The proof stress value may differ in different standards or applications. In German standard DIN, the prescribed plastic deformation is sometimes $e = 0.01$ (e.g. for austenitic steels), in British standard BS 0.001 or 0.005 and the American standard ASTM 0.002 or 0.001 [1]. It is important to mention, that for computational simulations, the proof stress approach for setting the elastic limit would not be sufficient. In the simulation, we are trying to describe the behaviour of material as close as possible. Therefore, the yield point describing the elastic limit must be the first point that deflects from the linear line.

The proof stress approach for setting the yield point does not always have to be used. For certain groups of materials (e.g. low carbon steels), the stress magnitude for plastic deformation initiation (i.e. initiation movement of dislocations) is significantly higher compared to the magnitude of propagating plastic deformation [3]. This phenomenon is called the yield point phenomenon or discontinuous yielding and it causes significant yield point elongation (depicted in Figure 3 d)). The upper point of this irregularity in the stress–strain diagram is the upper yield point s_{eH} , followed by the sudden drop to the heterogenous deformation at the constant stress [1], [3]. The last point of this heterogenous deformation is the lower yield point stress, s_{eL} . The identification of the yield point s_e is in this case simple – it is usually the lower yield point stress magnitude as the more conservative value. The reason for this behaviour are interstitial atoms, typically nitrogen and carbon. The dislocations, which cause the plastic deformation, are pinned to these interstitial solutes and are therefore immobile. Similar behaviour can be found in some polymers and superplastic metal alloys [1]. This phenomenon of discontinuous yielding is rather complex to describe in the following chapters (4. Identification of flow curve using the finite element method, 5. Application of chosen non-linear relationships) and was investigated in more detail in [2] and [4]. This thesis will furthermore investigate only curves without upper and lower yield points and discontinuous yielding (which fits given material 18CrNiMo7-6 – see chapters 4 and 5).

The ultimate tensile strength s_m is another important quantity. It is the maximum load divided by original undeformed cross-sectional area.

$$s_m = \frac{F_{max}}{A_0} \quad (3)$$

Until this point, the strain is uniform. The strain magnitude at the ultimate tensile strength is the engineering uniform strain e_u . Exceeding this point, the neck starts to appear on the specimen, in which the triaxial stress state occurs, and therefore stress components (axial σ_x , radial σ_y and circumferential σ_z) are non-uniformly distributed around its cross section [3]. The necking does not have to always appear. In that case, the ultimate tensile strength is equal to the stress magnitude at fracture (Figure 3 b) and c)).

The fracture point is the last point of the stress–strain curve.

The curve is called ‘engineering’, because the stress values are computed from the original undeformed cross-sectional area, and the strain is computed from the final elongation value. In reality, the cross-sectional area reduces, and therefore the true stress value increases. The engineering strain value e is approximately equal to the true strain value ε up to 2 % of its nominal value (see Figure 4) [3]. The engineering strain does not depend on the intermediate strains, but it is computed only from the final elongation value. The true strain, also known as logarithmic strain, is taking into account the series of increments by which the plastic deformation is being realised, and therefore describes the influence of a strain path more reliably compared to an engineering strain [5].

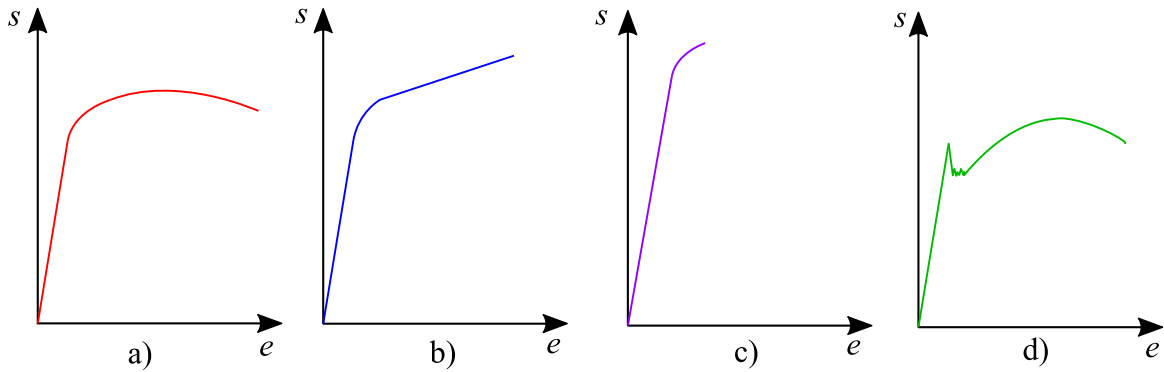


Figure 3 Depictions of typical engineering stress-strain curves: a) ductile material without yield-point elongation, b) material with plastic hardening without necking, c) brittle material, d) material with upper and lower yield point [2]

2.3. Additional tensile test outputs

Apart from force–elongation dependency, other important material constants are obtained from tensile test:

- Young’s modulus E , defined by T. Young in 1802. This constant describes the proportionality between stress and strain until the proportional limit (Figure 2). This material behaviour was described by R. Hooke in his well-known Hooke’s law:

$$s = Ee \quad (4)$$

- Poisson’s ratio ν , by which the materials ability of relative volumetric change within the region of elastic deformations is described. In the tensile test, ν is a ratio of transverse strain e_y (and e_z) to axial strain e_x [2].

$$e_y = e_z = -\nu e_x \quad (5)$$

- Engineering strain to fracture e_f , which is a measure of a material ductility (typically expressed in percentage), computed from the final length of deformed specimen L_f [1].

$$e_f = 100 \frac{L_f - L_0}{L_0} \quad (6)$$

- Reduction in area q , which is also a measure of ductility and it is computed in similar manner as elongation, only related to specimen’s areas:

$$q = 100 \frac{A_0 - A_f}{A_0} \quad (7)$$

E and ν are thus describing elastic properties. Quantities e_f and q are describing plastic properties and they are experimentally measured from the unloaded specimen's geometry after the fracture. Note that e_f depends on the gauge length L_0 . Hence for the same material and different specimen geometry, 2 different e_f values would be identified. Therefore, the gauge length should always be given together with the elongation results report [1].

2.4. True stress–true strain curve

The engineering stress and engineering strain are possible to recalculate up to the uniform strain into a true stress and true strain. True stress is defined as

$$\sigma = \frac{F}{A} \quad (8)$$

where A describes the instantaneous cross-sectional area of loaded specimen. The relationship between the engineering stress and true stress is

$$\sigma = s \left(\frac{A_0}{A} \right) \quad (9)$$

We assume that the increments of measured length are very small, and that they can be represented by ΔL_1 , ΔL_2 , ΔL_3 , etc. and the newly measured lengths are L_1 , L_2 , L_3 , etc. The overall strain can be computed from these increments as

$$\varepsilon = \frac{\Delta L_1}{L_1} + \frac{\Delta L_2}{L_2} + \frac{\Delta L_3}{L_3} + \dots = \sum \frac{\Delta L_j}{L_j} \quad (10)$$

If the sampling frequency of ΔL_j is fast enough, we can substitute the sum with an integral. Thus, the formula for true strain is

$$\varepsilon = \int_{L_0}^L \frac{dL}{L} = \ln \left(\frac{L}{L_0} \right) \quad (11)$$

where $L = L_0 + \Delta L$ is the instantaneous deformed length of the specimen. The relationship between the engineering strain and the true strain is

$$\varepsilon = \ln \left(\frac{L}{L_0} \right) = \ln \left(1 + \frac{\Delta L}{L_0} \right) = \ln(1 + e) \quad (12)$$

To be able to express the true stress from the outputs of a tensile test, the formula (9) needs to be rewritten as a function of load and elongation. This is done under the assumption that the change of shape in the plastic deformation is caused only by transferring mass in space – the volume remains constant. So, the specimen's volume $A_0 L_0$ remains constant throughout the test in the region of plastic deformation. We can write that

$$A_0 L_0 = AL \quad (13)$$

$$\frac{A_0}{A} = \frac{L}{L_0} = \frac{L_0 + \Delta L}{L_0} = 1 + e \quad (14)$$

hence

$$\sigma = s(1 + e) \quad (15)$$

Formulas (12) and (15) are used for recalculating the true stress and true strain from the tensile test. Note that these relationships are valid only until uniform strain. The goal of this thesis is to describe the true stress–true strain curve beyond the initiation of neck – the so-called flow curve.

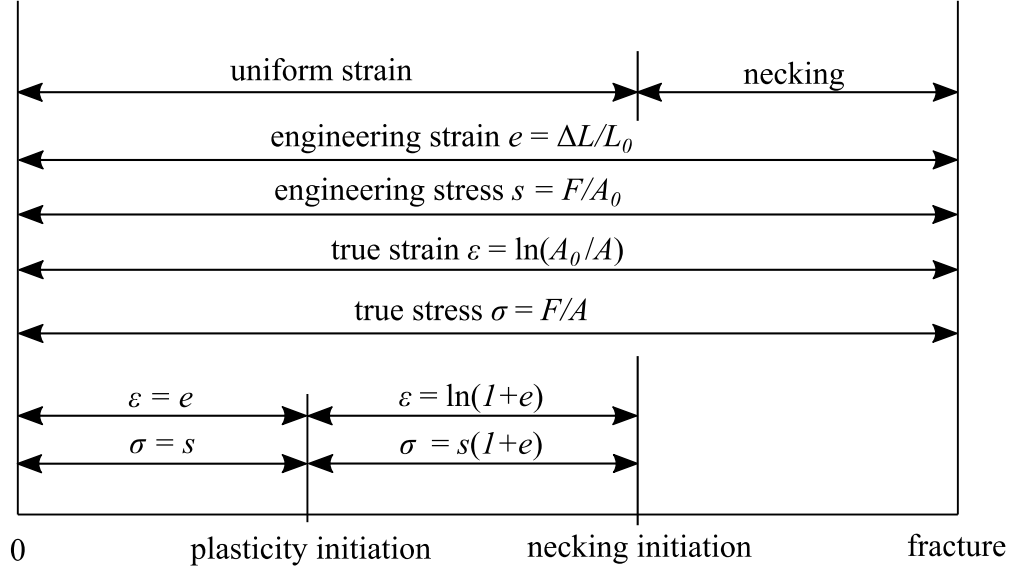


Figure 4 Engineering stress, engineering strain, true stress, true strain relationships and their range of validity. Modified from [3]

The engineering strain e is computed from the distance of two points, which are defining the length L_0 . When the stress exceeds the magnitude of ultimate strength s_m the so-called neck appears on the specimen. This region is called plastic instability. The magnitude of e describes the mean value of deformation in the necking area and does not correlate with deformation in the smallest cross-sectional area of the necking part [1]. There are additional methods that are used for the measurement of the instantaneous cross-sectional area in the necking part (i.e. Digital Image Correlation, measuring the necking area with additional sensors), however they are not standard equipment in the tensile test.

2.5. MLR Correction

Several correction methods, of how to gain flow curve after necking initiation appeared throughout history. Bridgman was the first, who carried out an analytical correction method. But, his correction method requires necking radius as an input and it is quite complicated to identify this quantity [6].

This method was further investigated by La Rosa and extended by Mirone in [7]. They developed following 4th order polynomial correction coefficient for stress and 3rd order polynomial correction coefficient for strain:

$$MLR_{\sigma} = 1 - 0.6058(\varepsilon_{eq,f} - \varepsilon_N)^2 + 0.6317(\varepsilon_{eq,f} - \varepsilon_N)^3 - 0.2107(\varepsilon_{eq,f} - \varepsilon_N)^4 \quad (16)$$

$$MLR_{\varepsilon} = 1 - 0.265(\varepsilon_{eq,f} - \varepsilon_N) + 0.241(\varepsilon_{eq,f} - \varepsilon_N)^2 - 0.074(\varepsilon_{eq,f} - \varepsilon_N)^3 \quad (17)$$

where $\varepsilon_{eq,f}$ is equivalent fracture strain:

$$\varepsilon_{eq,f} = 2\ln\left(\frac{d_0}{d_f}\right) \quad (18)$$

and ε_N is true strain at necking initiation.

The corrected average equivalent stress–strain curve beyond the necking initiation can be then computed:

$$\sigma_{eq,avg} = \frac{F}{A_f} MLR_\sigma \quad (19)$$

$$\varepsilon_{eq,avg} = \varepsilon_{eq,f} MLR_\varepsilon \quad (20)$$

In fact, these are coordinates of one point, which is connected with $[\varepsilon_N, \sigma_N]$ (the last point of analytically valid true stress–true strain curve from equations (12) and (15)) by a straight line. The demonstration of MLR correction is performed in chapter 4.2.

3. Non-linear stress–strain relationships

3.1. Constitutive elasto-plastic material model

To be able to perform computational simulations of elasto-plastic material, it is necessary to introduce a material model, which is defined analytically. The fundamental input for computational simulations is the true stress–true strain curve, the $\sigma = f(\varepsilon)$ dependency, the so-called curve of plastic hardening or flow curve. It is necessary to somehow mathematically describe experimentally obtained data from the tensile test within a satisfactory magnitude of deviation.

Some of the elasto-plastic material models are listed below:

- **Ideal**

This is the simplest elasto-plastic model, which does not include plastic hardening, the plastic part of curve is constant value of yield stress.

- **Bilinear**

Similar to the previous model, this model is described by 2 lines. In this case though, the plastic hardening is considered, hence the plastic part of curve is not constant, but a line with a slope. The ideal material model is hence a special case of the bilinear one, with a slope equal to zero in the second part of the curve.

- **Multilinear**

The multilinear material model describes $\sigma = f(\varepsilon)$ dependency with a piece-wise linear curve, divided into a finite number of lines. The creation of this model is simple, it is just a connection of a finite number of chosen key points on the experimentally identified true stress–true strain curve. By this approach, any shape of curve can be described. When pre-processing the simulation, the minimalization of the number of linear lines is desired to have an optimised simulation [2].

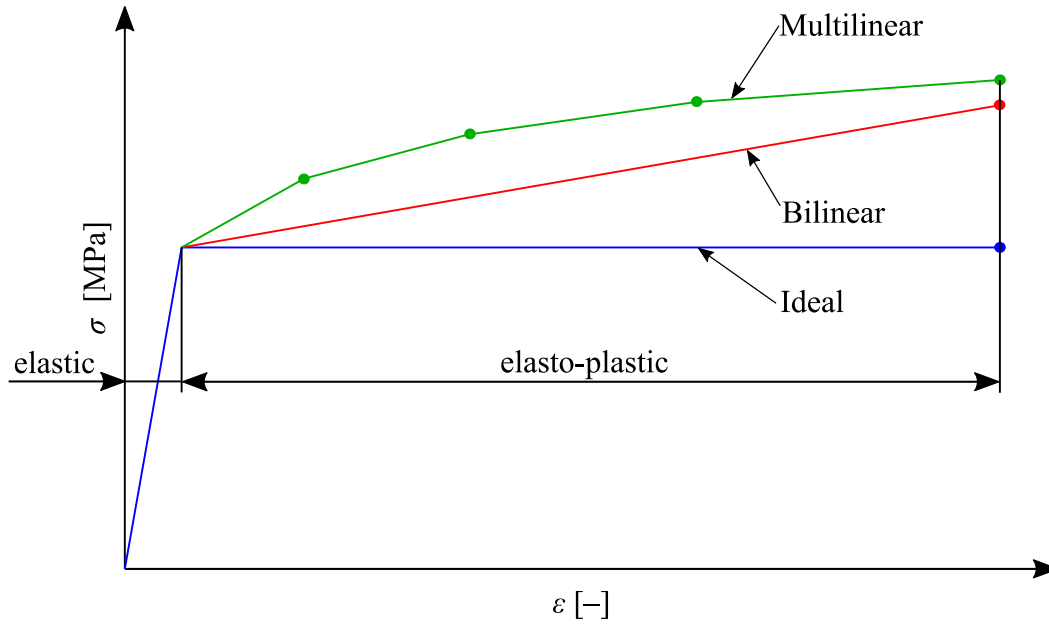


Figure 5 Examples of piece-wise linear material models. Modified from [2]

- **Non-linear**

Several empirical mathematical relations have appeared throughout history. This frequently used approach allows describing the plastic part of the curve by certain parameters [2], [8]. Many of these relations were dedicated to certain material group, therefore their applicability is limited and not versatile.

Table 1 Summary of some of the frequently used relations, described in this thesis

Name	Equation	No. of parameters	Chapter
Hollomon	$\sigma = K_H \varepsilon_{pl}^{n_H}$	2	3.2
Ludwik	$\sigma = \sigma_0 + K_L \varepsilon_{pl}^{n_L}$	2	3.3
Swift	$\sigma = K_S (\varepsilon_{pl} + \varepsilon_0)^{n_S}$	3	3.4
Voce	$\sigma = B_V - (B_V - A_V) e^{-n_V \varepsilon_{pl}}$	3	3.5

3.2. Hollomon

The equation is [9]:

$$\sigma = K_H \varepsilon_{pl}^{n_H} \quad (21)$$

where ε_{pl} is true or equivalent plastic strain, n_H strain hardening exponent and K_H is a constant, sometimes called strain hardening (or strength) coefficient [10]. This relationship was defined by J. J. Hollomon in 1945 in [9] and it is the most widely used one. The description of material hardening by n_H is convenient and can also be used for the assessment of stretch-formability and other technological aspects [8].

Let's take a closer look at the formula and the solution of its parameters. The formula can be expanded by adding logarithms on both sides:

$$\log(\sigma) = n_H \log(\varepsilon_{pl}) + \log(K_H) \quad (22)$$

which is in log-log coordinates equation of a line ($y = kx + q$). Thus, the unknown parameters K_H and n_H can be easily identified by fitting linear line in log-log coordinates – K_H is equal to intercept of the linear line in log-log coordinates at $\varepsilon_{pl} = 1$ and n_H is the slope of this curve [10]. Note that this is done in equivalent (or true) stress–equivalent plastic strain coordinates. The method of least squares is exclusively used for curve fitting [2].

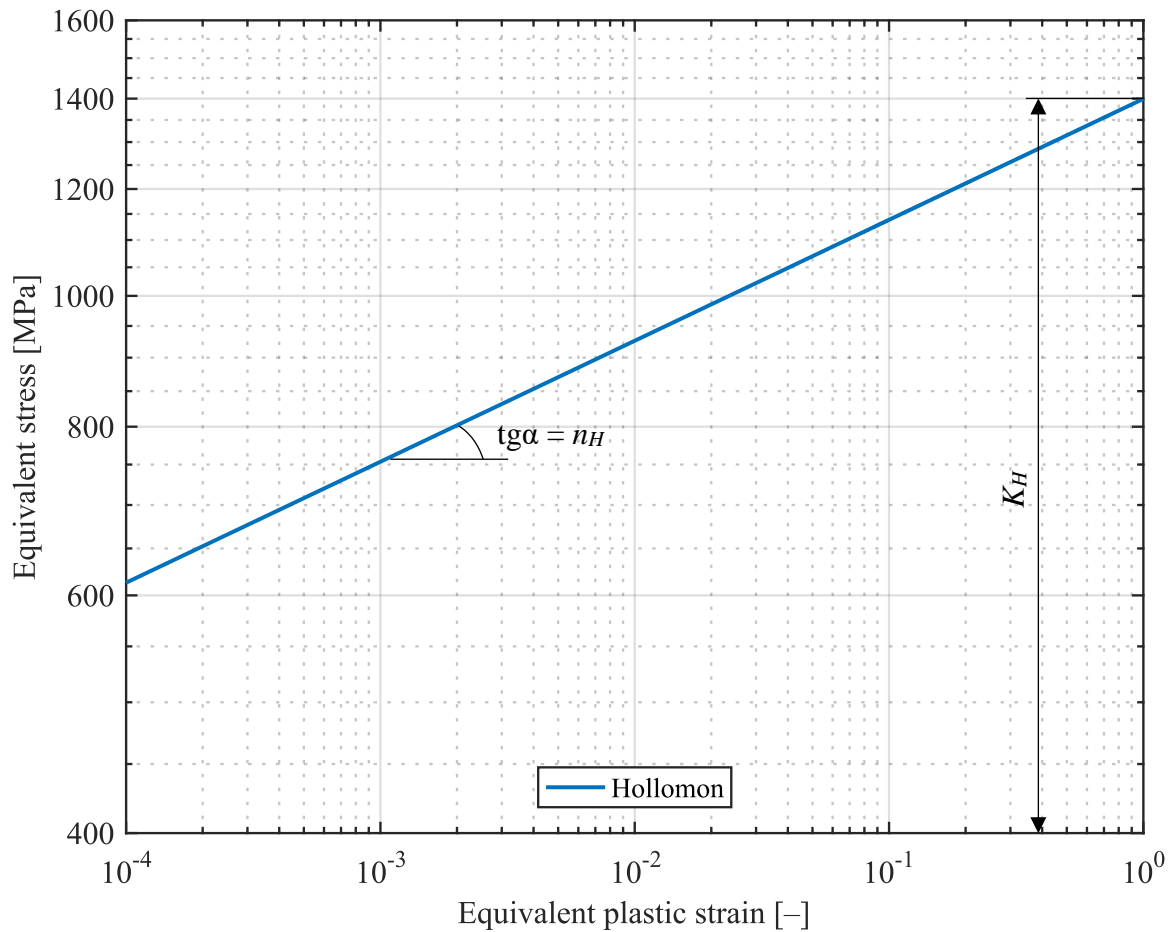


Figure 6 Example of Hollomon's relationship plotted in log-log coordinates. Modified from [10]

As mentioned, the hardening parameters K_H and n_H have a technological importance. The K_H value gives some idea of the strength level of a material as well as the magnitude of forces that are required for its forming. The n_H value describes the strain hardening characteristic. The greater the magnitude of n_H , the greater is the material's strain hardening rate. If we seek a material for processes that are realised by plastic deformation, the material with higher magnitudes of n_H is more suitable and should be preferred. Also, the stretch formability can be described by the n_H parameter. The magnitude of n_H affects the location of uniform strain,

hence the greater the n_H value, the more the material can plastically deform before necking and plastic instability occur [10].

The n_H value in some cases correlates with the value of the true uniform strain ϵ_u . This was investigated by Kleemola in [8]. He was comparing the fit of the Hollomon's relationship with other non-linear relationships, summarizing their correlation. He was also fitting the relationships from Table 1 into experimental data and investigating their correlation and deviation of the n_H value from ϵ_u . Finally, he investigated the influence of the strain increment on the fit. He stated that *"short strain increments can be very accurately described by the Hollomon expression, but then the exponent does not give the correct uniform strain. Only when the strain increment is sufficiently small and contains the actual uniform strain point does the Hollomon exponent approximate the value of ϵ_u . However, it is not known beforehand what the correct strain increment is."* The examination of correlation of n_H and ϵ_u was performed experimentally in this thesis – see chapter 5.2.

Hollomon's relationship is generally more suitable for materials with higher magnitudes of plastic strain [10].

3.3. Ludwik

P. Ludwik's relationship from 1909 is [8]

$$\sigma = \sigma_0 + K_L \epsilon_{pl}^{n_L} \quad (23)$$

Similar to Hollomon's relationship, the stress is a power law of plastic strain. In this case though, the value of yield point stress is taken into account and represented by the parameter σ_0 . The n_L defines curvature of the curve in log-log coordinates, whilst K_L represents the intercept of this curve.

The modification of Ludwik's relationship into log-log coordinates is as follows. Firstly, σ_0 is moved to the left side. Then, logarithms are applied on both sides and the equation is modified to [8]:

$$\log(\sigma - \sigma_0) = n_L \log(\epsilon_{pl}) + \log(K_L) \quad (24)$$

Since there are only 2 unknown parameters (n_L and K_L), the coefficients are easily identified by using the least square method.

The Figure 7 bellow shows the difference between Hollomon's and Ludwik's fit applied on experimentally measured data. Ludwik's relationship is non-linear in log-log scale, when compared to Hollomon's linear one. The difference is caused by the influence of σ_0 .

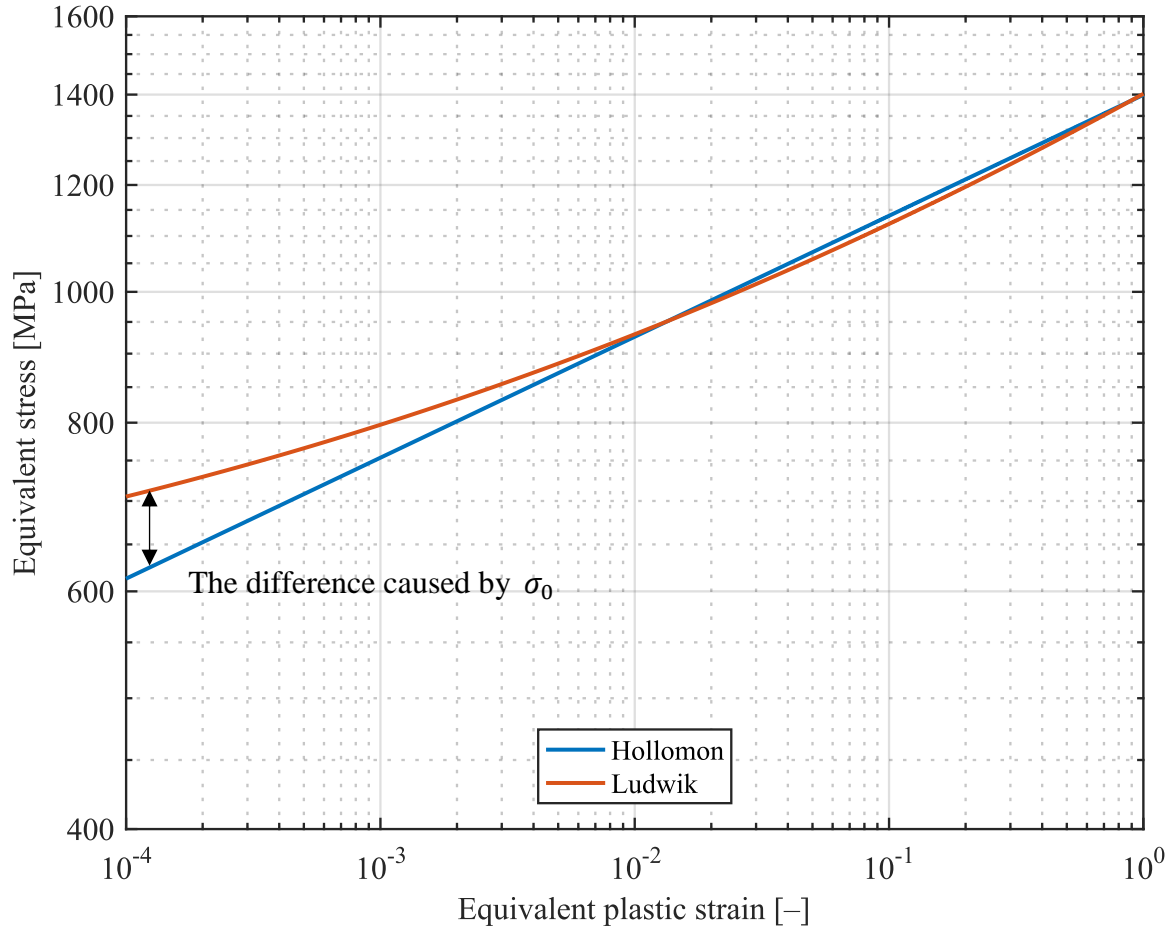


Figure 7 The difference between Hollomon's (3.2) and Ludwik's fit. Modified from [10].

3.4. Swift

The equation defined by H. W. Swift in 1952 is [11]:

$$\sigma = K_S(\varepsilon_{pl} + \varepsilon_0)^{n_s} \quad (25)$$

In this relationship, a constant strain value ε_0 is present, similar to σ_0 in Ludwik's formulation. All three parameters are unknown and need to be identified using the non-linear least square fit.

The estimation of the values of initial guesses is a critical part of least square fitting procedure. That is because the non-linear system does not always have an unambiguous solution (in fact the number of solutions depends on the fitted function, the number of solutions can be up to infinity). It is necessary, to be able to have an educated initial guess, otherwise the solution might converge only to the local minimum of the least square error, but not towards to global

minimum¹. Figure 8 depicts Swift's relationship plotted together with previous relationships. In case of this dataset, Swift gives a very similar fit to Hollomon's.

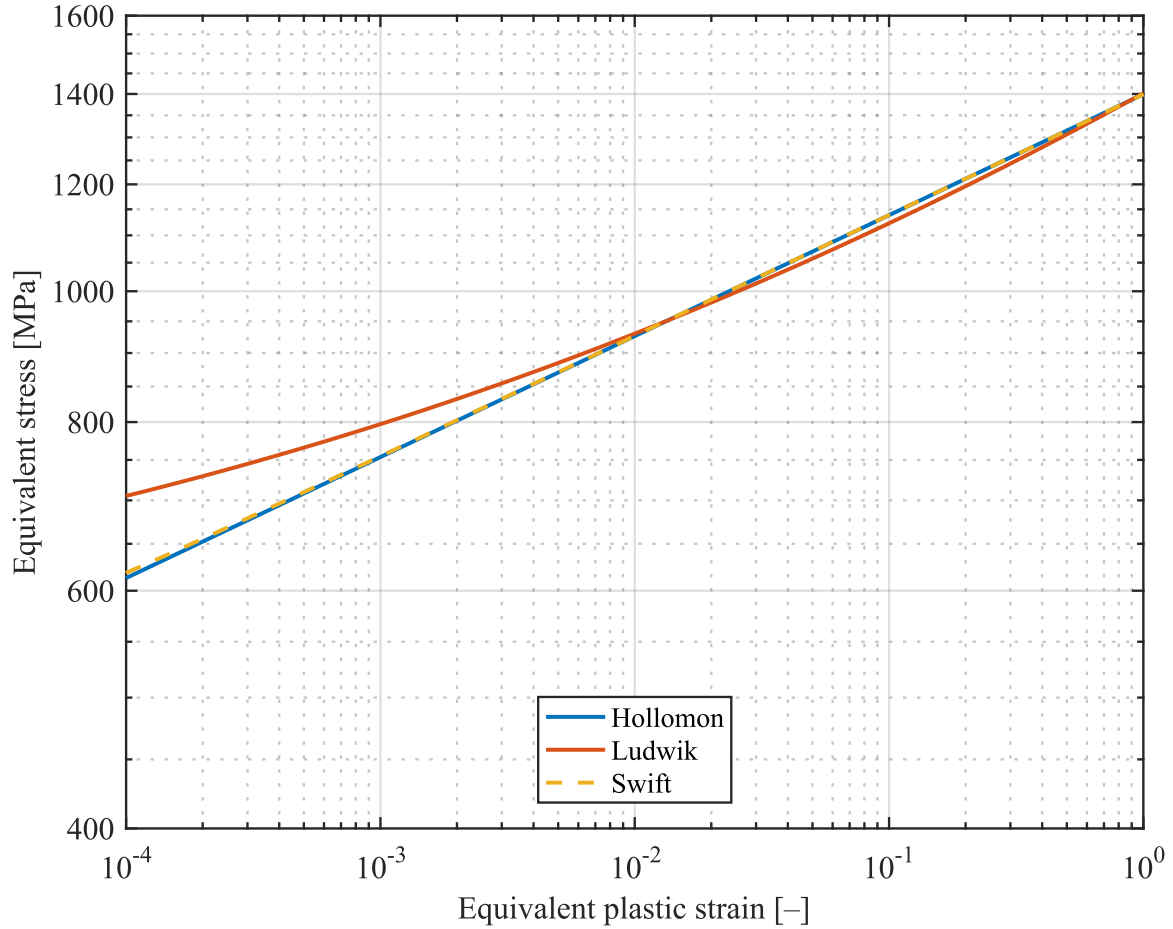


Figure 8 Comparison of Hollomon, Ludwik and Swift fit in log-log coordinates, fitted to the same dataset.

3.5. Voce

The equation defined by E. Voce in 1948 is [12]:

$$\varepsilon_{pl} = K_V \ln \left(\frac{B_V - A_V}{B_V - \sigma} \right) \quad (26)$$

where A_V is the initial or threshold stress at which homogenous plastic deformation begins to be appreciable. B_V is the final constant stress, attainment of which at indefinitely large strains appears to be a characteristic of homogenous deformation. The K_V is a dimensionless constant [12].

¹ Paraphrased from J. N. Kutz's online lecture *Data Fitting with Matlab*, University of Washington, Department of Applied Mathematics. Available online (youtube.com), or in study text: Kutz, J. N.: *AMATH 301 Beginning Scientific Computing*. Seattle: University of Washington, Department of Applied Mathematics. 2003.

The expression of stress as a function of strain from equation (26) is [8]:

$$\sigma = B_V - (B_V - A_V)e^{-n_V \varepsilon_{pl}} \quad (27)$$

where n_V is a dimensionless exponent, equal to K_V^{-1} , which gives a value of saturation rate.

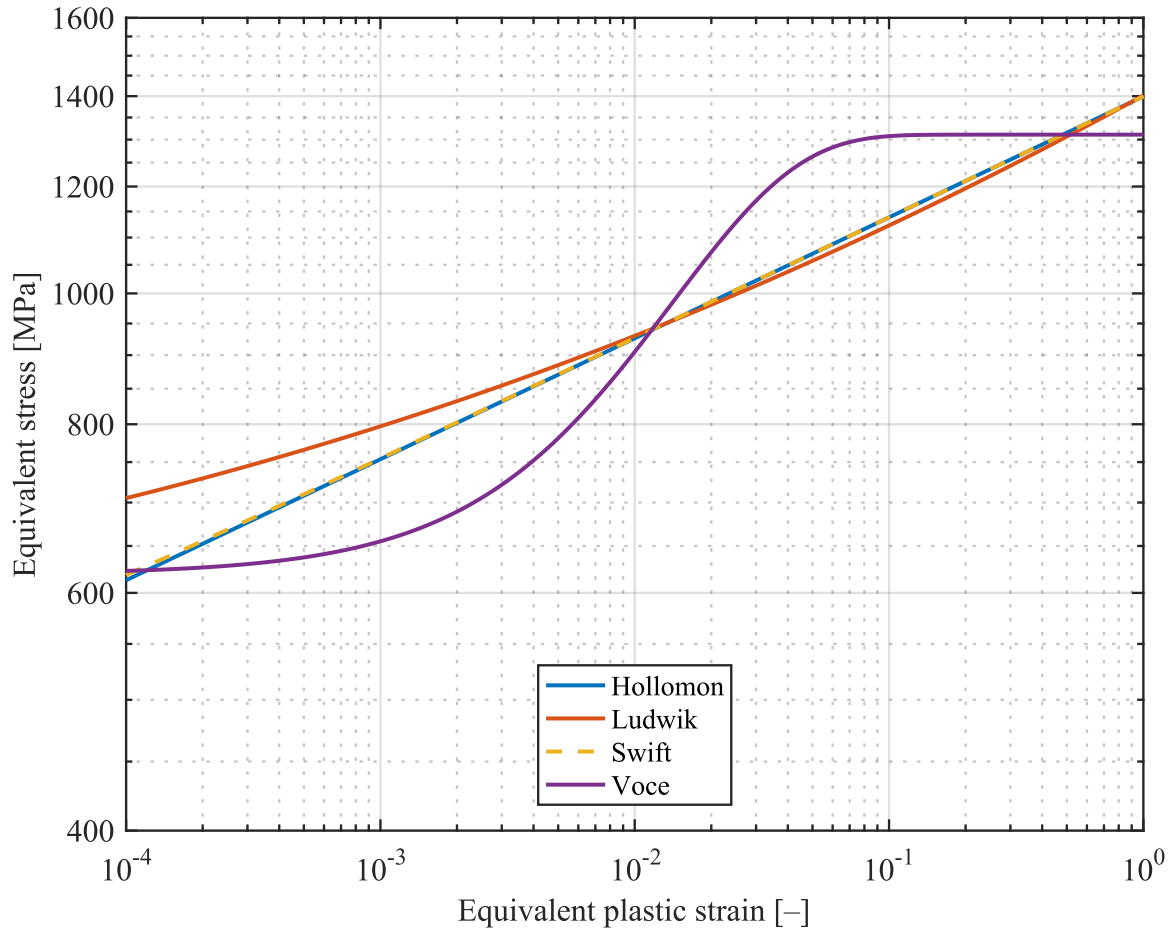


Figure 9 Voce's relationship fitted to the experimental dataset over previous relationships

Voce was proposing this relationship, after investigation done on various non-metallic alloys, such as copper, brass, bronze, etc. He stated that the constant A_V is usually above the limit of proportionality and roughly corresponds with proof stress for 0.1 % of strain [12]. The correlation of these quantities was examined on experimentally performed fit - see chapter 5.2.

4. Identification of flow curve using the finite element method

4.1. Introduction

The experimental tensile test of 18CrNiMo7-6² was provided by the supervisor Ing. František Šebek, Ph.D. The test was performed at room temperature in the laboratory of the Institute of Materials Science and Engineering. The load–elongation output was received in digital form for post-processing. Apart from the output, the rest of the measured quantities is listed below:

$$s_{p0,2} = 738 \text{ MPa}$$

$$s_m = 1053 \text{ MPa}$$

$$E = 196 \text{ GPa}$$

$$A_0 = 29.03 \text{ mm}^2$$

$$A_f = 12.63 \text{ mm}^2$$

$$L_{0ext} = 30 \text{ mm},$$

where A_f is the area of the specimen at fracture.

4.2. Stress–strain curves

The engineering stress–strain curve can be plotted instantly, converting measured values using equations (1) and (2). Similarly, the analytically computed true stress–true strain curve can be plotted using equations (15) and (12), but only until the necking initiation, as described in chapter 2.4.

The MLR correction can be directly performed as well to estimate the average equivalent stress trend beyond necking, following the procedure described in chapter 2.5.

² Case hardening steel according to DIN EN 10084, with chemical composition of chrome 1.50-1.80 %, nickel 1.40-1.70 % and molybdenum 0.25-0.35 %. Information found in online catalogues of companies Saarlust AG and Gruppo Lucefin S.p.A.

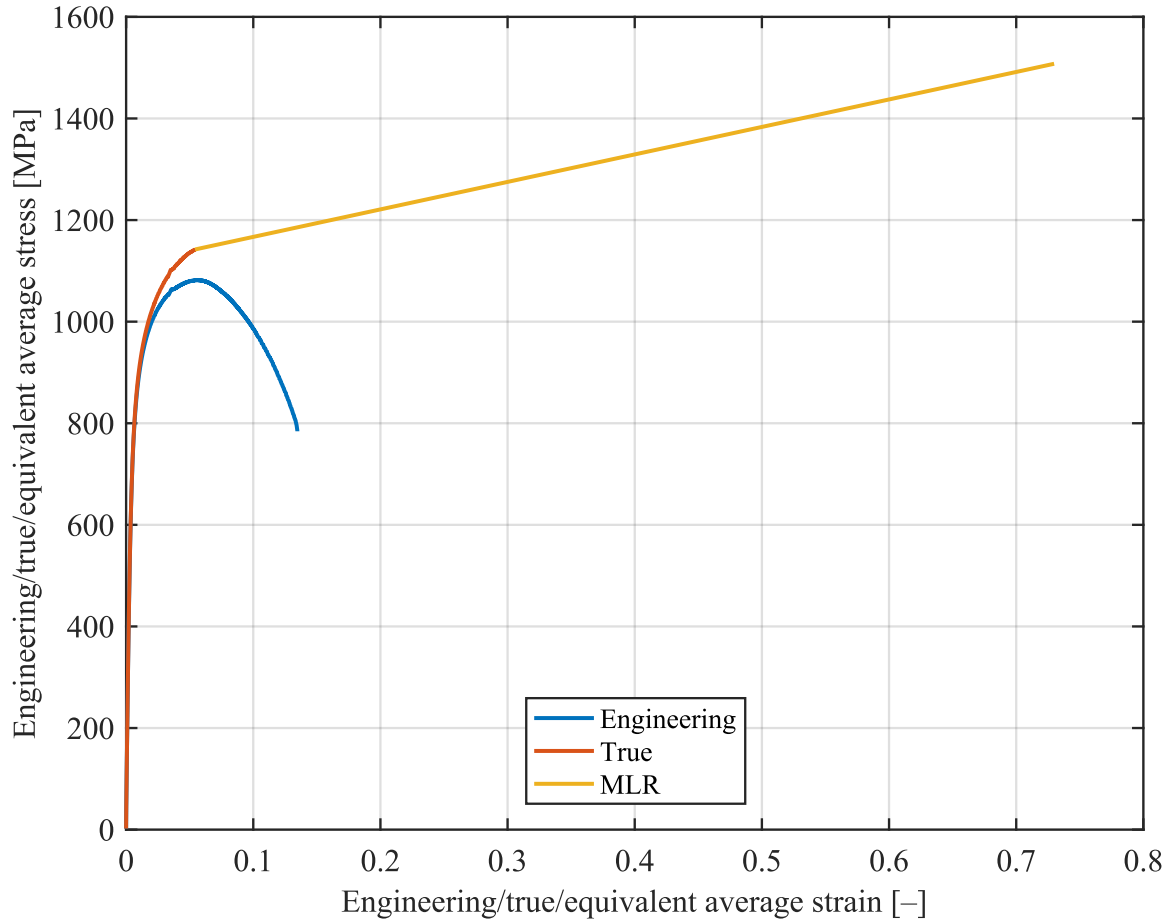


Figure 10 Stress–strain curves directly plotted from experimental measurement

4.3. Flow curve calibration and tensile test finite element simulation

As it was mentioned before, the stress–strain curve serves as an essential input into numerical simulations. For cases with large-scale deformations, e.g. plastic flow localization, metal forming or ductile crack propagation, the MLR correction does not sufficiently describe the plastic behaviour of material [4].

In this thesis, an iterative finite element method in the ANSYS analysis system is presented. It is an iterative process, wherein each iteration material input is modified. The modification is based upon manual comparison of the reaction force response from the simulation to an experimentally measured force.

The tensile test is modelled as a axisymmetric problem. The symmetry allows us to simplify the geometry.

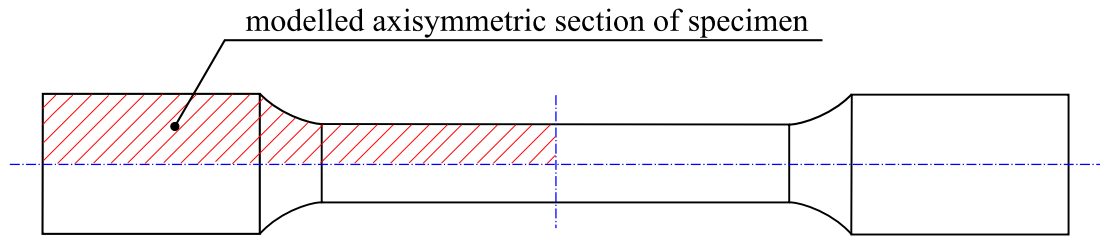


Figure 11 Simplified geometry of tensile test specimen

Jeník stated in [2], that if the tensile test was realised in the presence of an extensometer, it is unnecessary to take in account the clamping part of the specimen, and it is possible to simplify the geometry even more as in the following Figure 12:

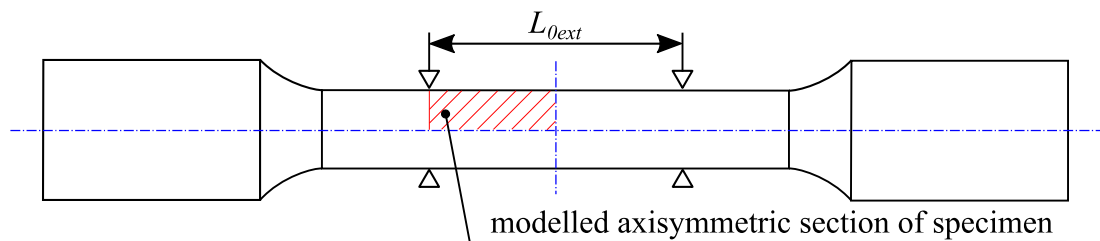


Figure 12 Simplified geometry of tensile test specimen with extensometer

The mesh was done using quadratic element PLANE183. The size of the elements was chosen in such a way that there were 15 elements over the radius of section. This was done based on Jeník's study, who performed a sensitivity analysis of mesh refinement [2]. He learned, that even the difference between 15 and 9 elements per radius in terms of equivalent stress was less than 0.5 % in his case. 15 elements per radius should be sufficient enough in this case.

Since we are modelling a perfectly cylindrical section of the specimen, it is necessary to create imperfection to assure necking. The radius has been reduced by 3 ‰. That assures the initiation of plastic instability in the desired place – Figure 13. Otherwise the deformation would be linear throughout the cylindrical section, if the imperfection was not created. The creation of neck can be seen in chapter 4.3.2.

The problem was solved using a macro in Ansys Parametric Design Language (APDL) in ANSYS Mechanical APDL 18.1 software. The APDL macro guarantees maximal parametricity.

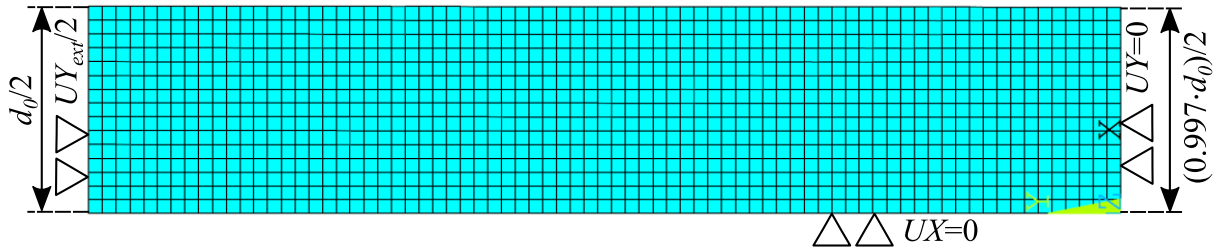


Figure 13 Meshed axisymmetric model with depicted boundary conditions

4.3.1. APDL Macro

The created APDL macro needs two text files as an input – the input is the estimated flow curve – *fl_eps.txt*, which consists of the equivalent strain coordinates, and *fl_sig.txt*, which consists of the equivalent stress coordinates. The input must be formatted to be in two separate columns, with the serial number in the first column and the corresponding value in the second one.

!APDL PIECEWISE LINEAR FLOW CURVE IDENTIFICATION MACRO

!Josef Kostal, Bachelor's thesis, Brno 2018

FINISH

/clear

!Definition of parametres

displ = 2	<i>!Displacement (divided by 2 due to symm.)</i>	<i>[mm]</i>
nl = 40	<i>!Number of loadsteps</i>	<i>[-]</i>
pt = 19	<i>!Number of points of flowcurve</i>	<i>[-]</i>
el = 0.2	<i>!Length of element</i>	<i>[mm]</i>
rs = 3	<i>!Radius of the specimen</i>	<i>[mm]</i>
l0ext = 15	<i>!l0ext = L0ext/2 - half of the length L0ext</i>	<i>[mm]</i>
mu = 0.3	<i>!Poisson's ratio</i>	<i>[-]</i>

Figure 14 Input parameters of the macro

It is reasonable, to base the first estimation of stress–strain input on MLR correction.

The other input parameters are in Figure 14. It is necessary to align the number of points of the flow curve *pt* with the highest serial number from *fl_eps.txt* (and *fl_sig.txt*).

Macro then solves the problem in a number of loadsteps *nl* that was inserted, and in each loadstep the reaction force F_y is written into output. The output file *feedback.dat* contains force–elongation data from the simulation.

The output is then compared with the experimental measurement. Note that the displacement data from *feedback.dat* needs to be multiplied by 2 due to symmetry. The user then checks the deviation between the FEM simulation and the experiment. This can be done by created MATLAB script *comparison.m*, which is included in the attachment. Based on the deviation,

the input data of *fl_eps.txt* and *fl_sig.txt* can be modified and a new iteration computed.

The created macro *macro.mac* can be found in the attachment of this thesis, as well as the material input of the 26th iteration *fl_eps.txt* and *fl_sig.txt* and a simulation output *feedback.dat*. The experimentally measured tensile test of given steel is also included – *experiment.dat*

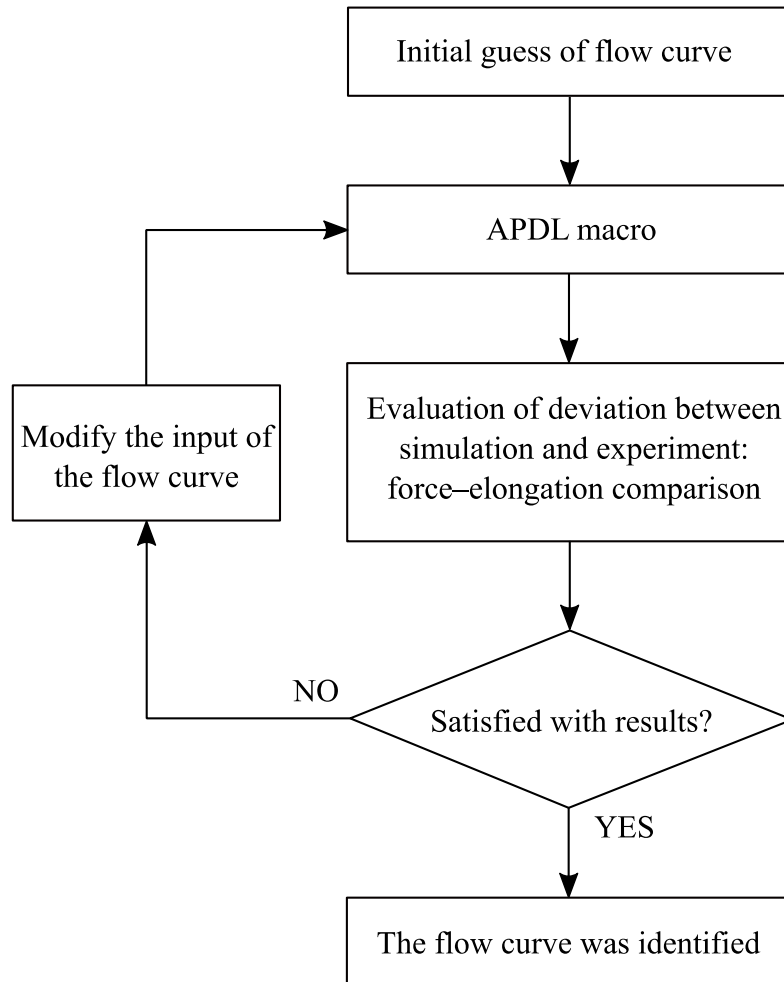


Figure 15 Flowchart of iterative finite element method of the tensile test simulation

4.3.2. Results

The simulation was run 26 times to identify the flow curve. The first part of the flow curve input was analytically computed (in the uniform strain region) using the equations 12 and 15, and the rest of the curve was modified and calibrated until the resulting deviation between the simulation and experiment was satisfying.

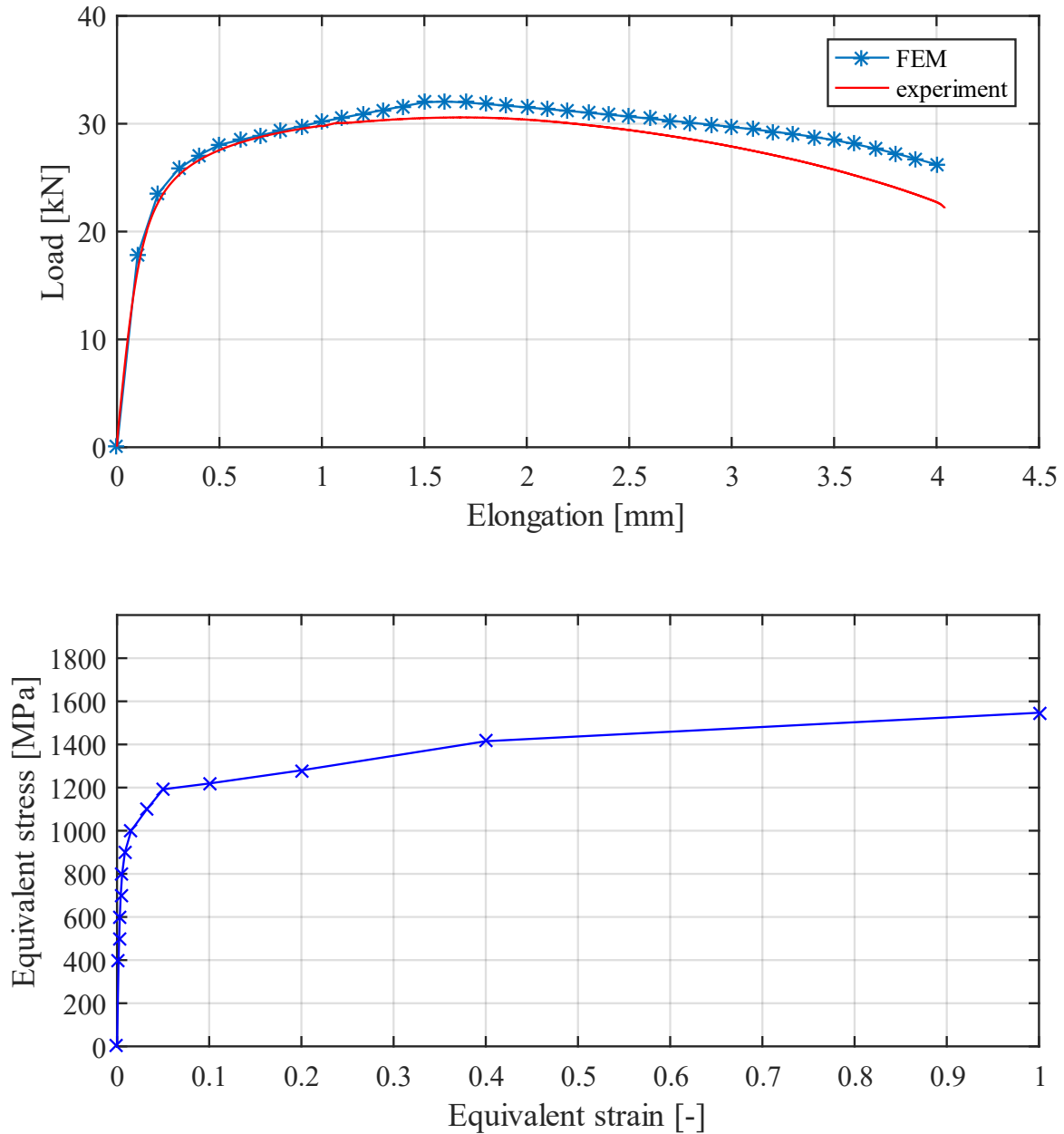


Figure 16 The results of 5th iteration

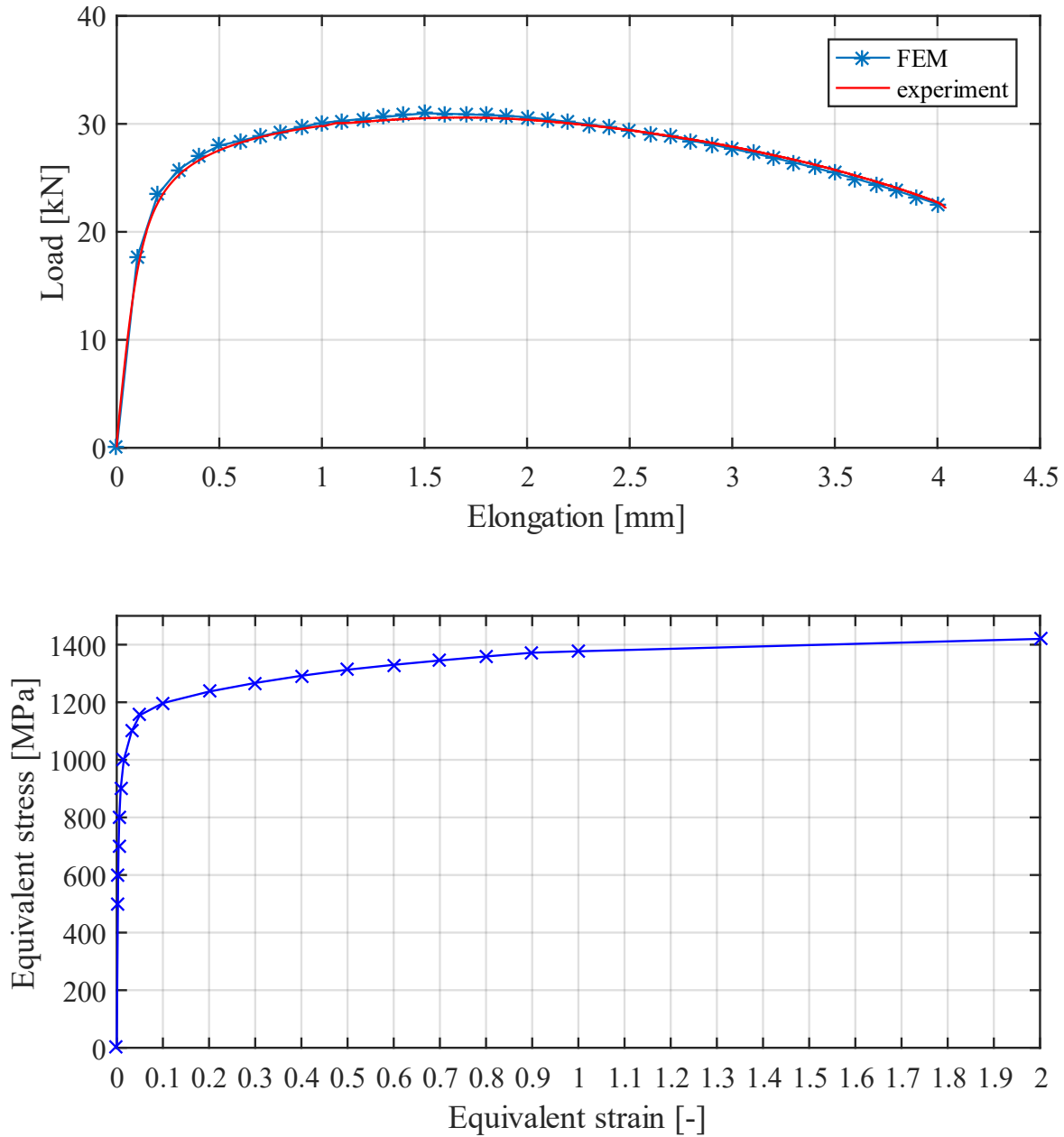


Figure 17 The results of 26th iteration which are satisfactory to the author

The flow curve was identified, so the slope of the curve is decreasing in each evaluated strain point. The percental difference between the experiment and the simulation is lower than 1.5 % in the whole region of plastic instability – the *table.pdf* with the percental difference is in the electronic attachment and also printed on the last page of this thesis. In fact, the whole force–elongation curve from simulation was not differing more than 1.5 % from the experiment, except for the first 5 elongation points. However, these 5 points with higher percental difference are dependent on analytically computed part of the flow curve, and understandably, the highest difference is on the yield point – 8.19 %. That is, because in the vicinity of the yield point the force rises dramatically with relatively small elongation increment. The goal of this thesis was primarily to calibrate the curve in the region of plastic instability.

The percental difference d_{sim} from *table.pdf* was calculated using the following formula:

$$d_{sim} = 100 \left| \frac{F_{exp} - F_y}{F_{exp}} \right| \quad (28)$$

where F_{exp} is force measured in the tensile test.

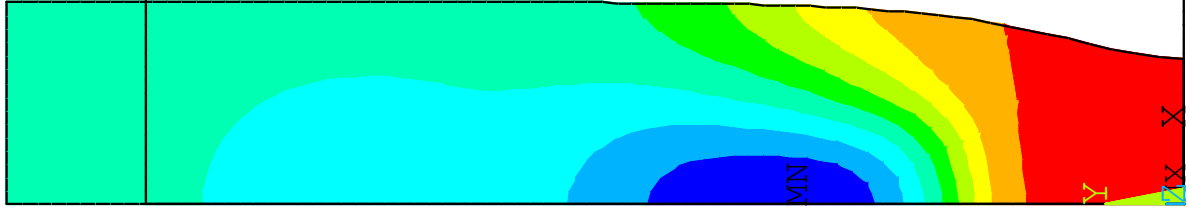


Figure 19 The necking appearance at the end of the simulation

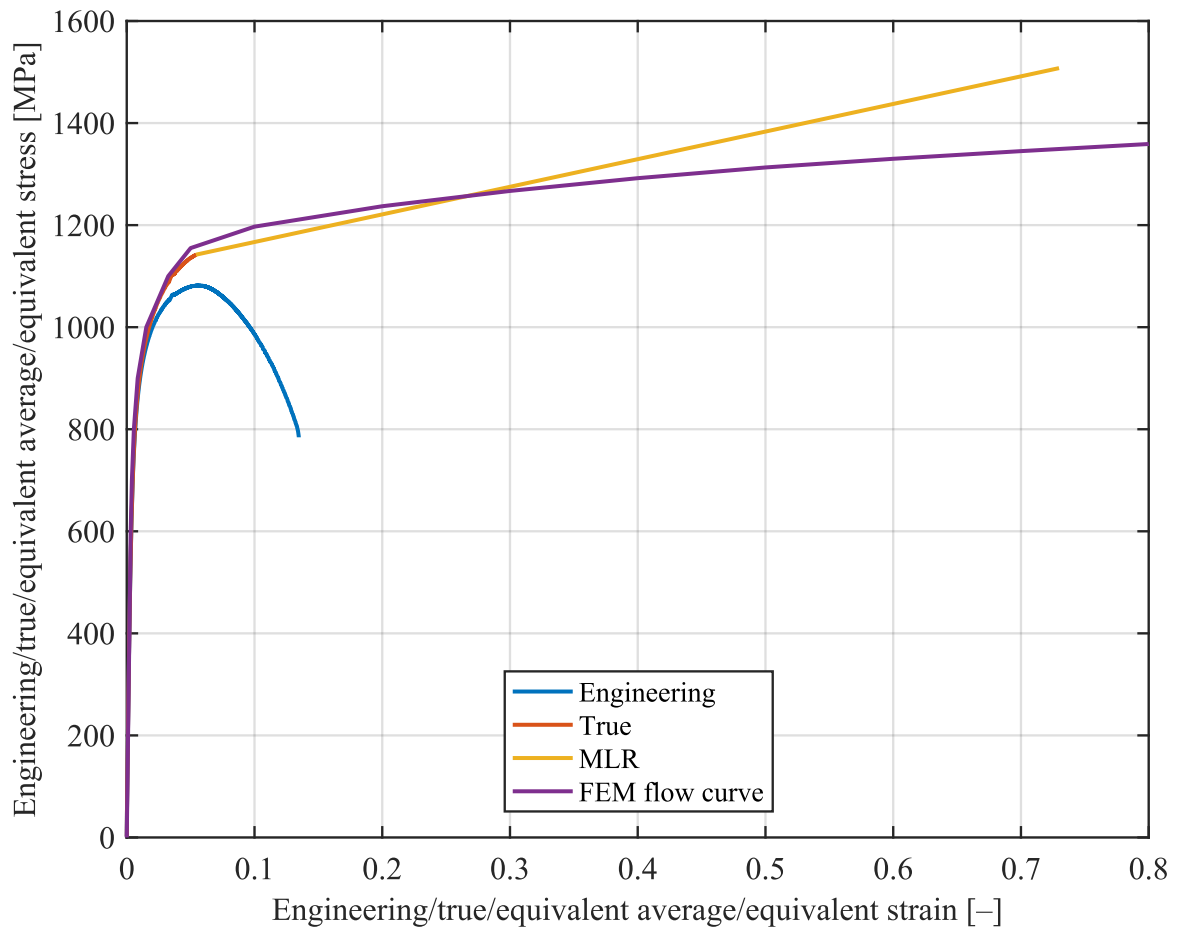


Figure 18 Comparison of identified stress–strain curves

5. Application of chosen non-linear relationships

The relationships from Table 1 were fitted to the identified flow curve from chapter 4. A user interface was designed for curve fitting.

5.1. The user interface

The user interface code *fitting_GUI.m* was developed in MATLAB, version R2016a. It follows the logic of inputs of previous APDL macro (4.3.1), thus it automatically loads the calibrated flow curve from *fl_eps.txt* and *fl_sig.txt* from the working directory – these input files need to be in the same folder as the user interface code together with *fitting_GUI.fig* (graphical environment of user interface).

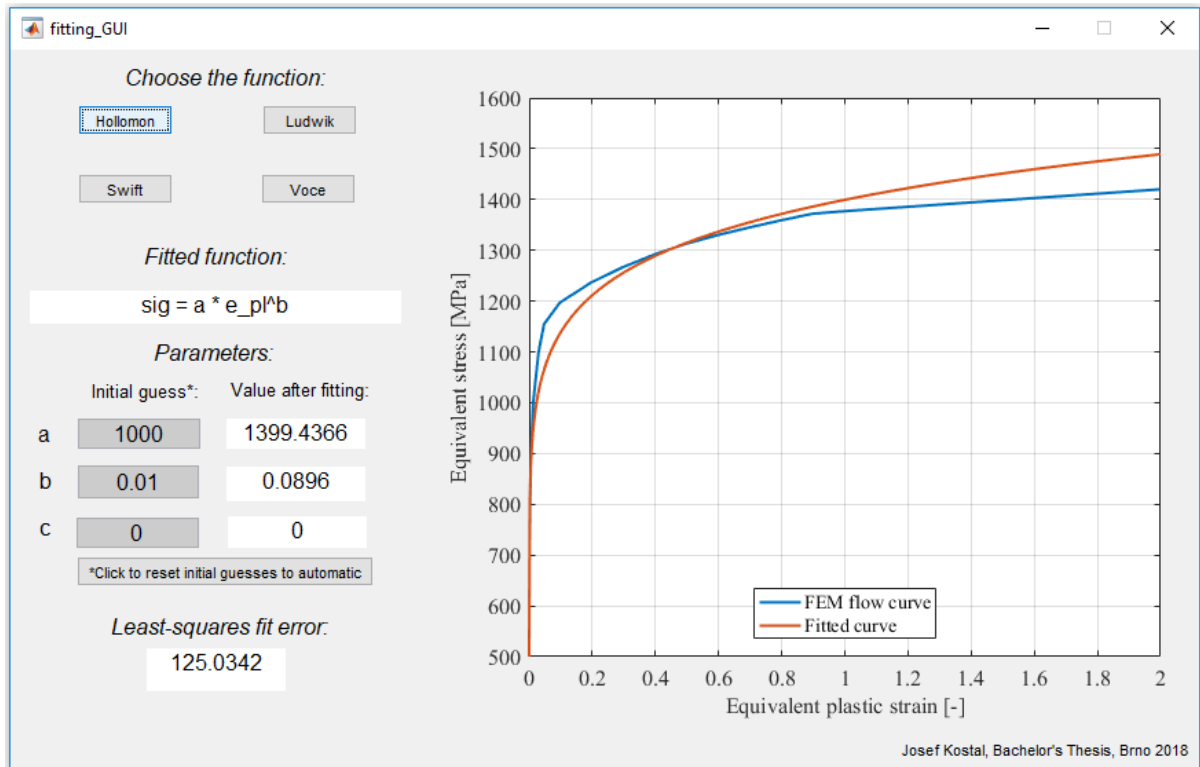


Figure 20 The environment of created interface, depicting Hollomon fit

The interface contains four buttons with functions from Table 1 and three editable text boxes of initial guesses.

The user then simply inputs the initial guesses of parameters into the grey boxes and clicks the button of the function that was chosen to fit. The box with the caption “*Fitted function*” shows which function was fitted and the three white boxes with static text show the value of the parameters after least square fitting. The least square fit error Er (also known as root-mean square error) is computed:

$$Er = \sqrt{\frac{1}{pt} \sum_{i=1}^{pt} |\sigma_{fit,i} - \sigma_{flow\ curve,i}|^2} \quad (29)$$

where σ_{fit} is equivalent stress value of fitted curve and $\sigma_{flow\ curve}$ is equivalent stress value of identified calibrated flow curve. As mentioned in chapter 3.4, the initial guess is a critical part of fitting a non-linear relationship using the least square method. When the inaccurate values are inserted, the solution can converge only to the local minimum of the least square error.

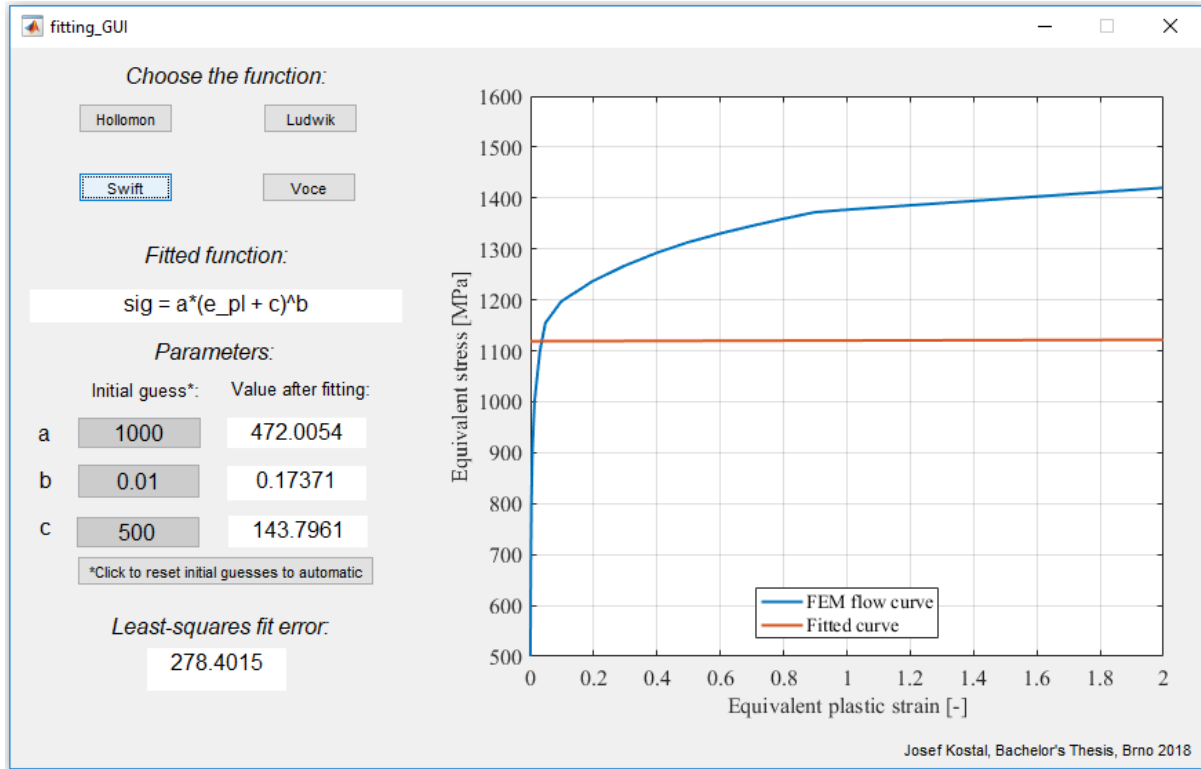


Figure 21 Typical example of inaccurate input of initial guesses, leading to the bad fit

An additional reset button was developed for this study. The button with the text “*Click to reset initial guesses to automatic” resets the values of initial guesses to zeros. If the user then clicks the button with function again, a new set of initial guesses is automatically inserted. Any zero inserted as an initial guess is converted to the automatic value of initial guess. It is important to emphasise, that these automatically inserted initial guesses were designed for this specific case of 18CrNiMo7-6 steel using a method of trial and error. They do not have to assure the convergence to the global minimum of least square fitting error, if a different flow curve is inserted. But, the user can modify initial guesses directly and insert own educated initial guesses for a specific case.

The limit for initial guess for all the exponents was set, so the number cannot be infinite. If the magnitude of the exponent was exceeded, a message box displays, and the value of the exponent restores the automatic value.

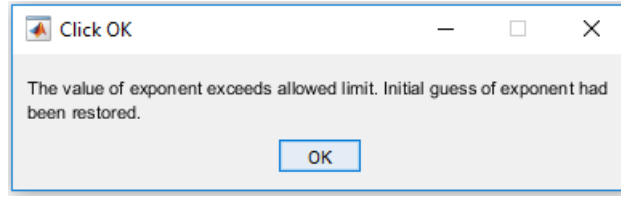


Figure 22 A message box, displayed when the exponent value exceeds the limit

5.2. Results of fitting

The best fit was found using Swift's relationship (chapter 3.4), giving the lowest least squares fit error of 49.9.

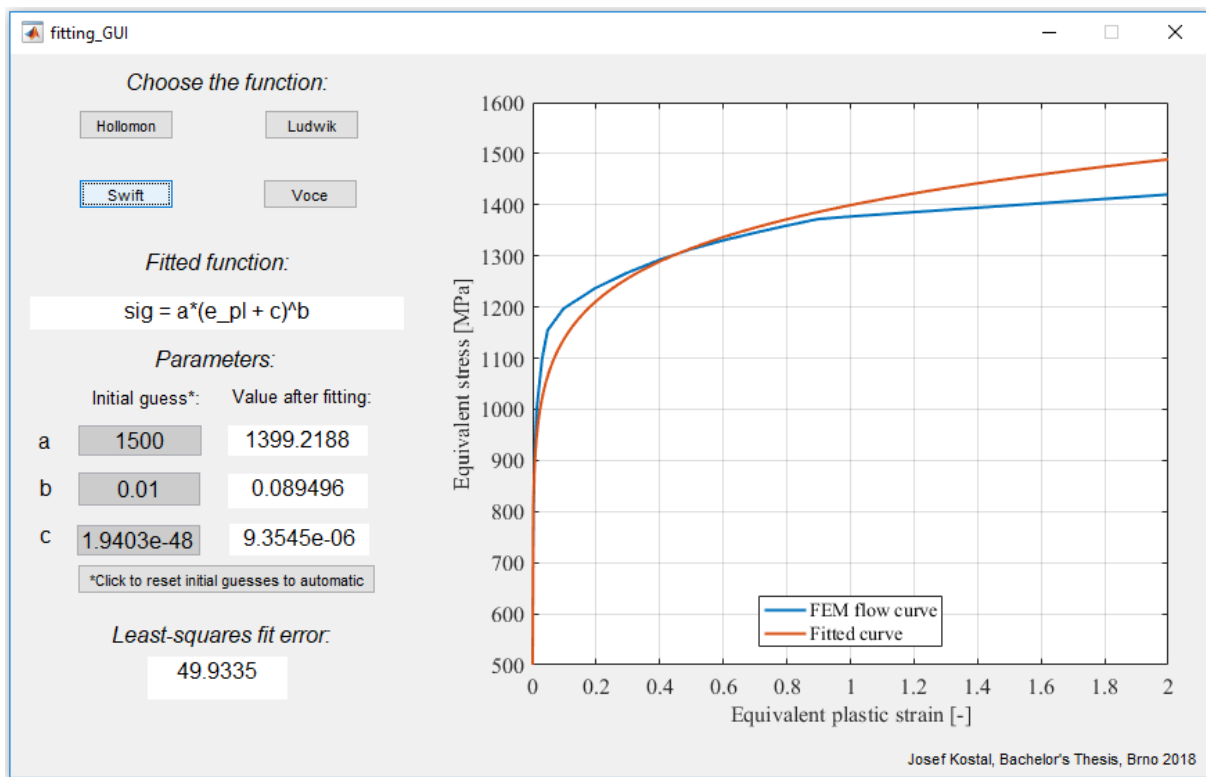


Figure 23 Swift fitted to the calibrated flow curve

Note that Hollomon gives a very similar fit with much higher error. That is caused by the fact that in the initial point, where the flow curve's equivalent plastic strain is equal to zero and equivalent stress is equal to yield point stress, Hollomon gives the value of equivalent stress of zero instead of yield point stress. That is because of the formulation of Hollomon's relationship. It is questionable whether or not Hollomon really is a function of equivalent plastic strain and not a function of equivalent total strain and whether it can be used like that.

In this case of 18CrNiMo7-6 calibrated flow curve, the found parameters of fitted Hollomon's relationship are:

$$\sigma = 1399.4 \cdot \varepsilon_{pl}^{0.0896} \quad (30)$$

in which if we input the value of strain $\varepsilon_{pl} = 0.00001$

$$\sigma = 1399.4 \cdot 0.00001^{0.0896} = 498.8 \text{ MPa} \quad (31)$$

which corresponds with the identified value of yield point stress 500 MPa. Thus, we can say that Hollomon's relationship contains the point [0;0], but if the input of equivalent plastic strain is higher than $1 \cdot 10^{-5}$, the relationship fits plastic coordinates.

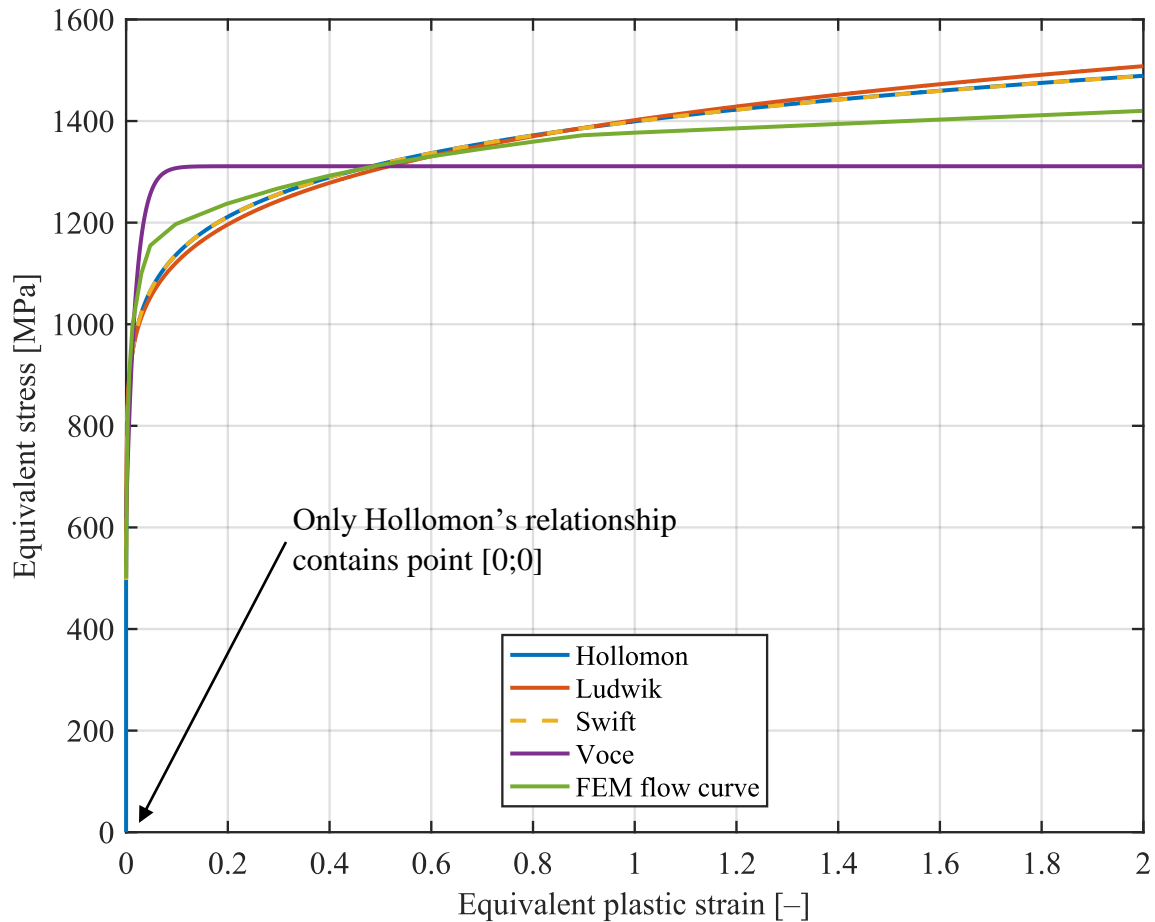


Figure 24 Stress–strain curves comparison

Identified parameters and errors of fitted functions are in Table 2 bellow.

Table 2 Identified parameters of chosen non-linear relationships

Hollomon	Ludwik	Swift	Voce
$Er = 125.03$	$Er = 65.82$	$Er = 49.93$	$Er = 69.32$
$K_H = 1399.4 \text{ MPa}$	$K_L = 901.8 \text{ MPa}$	$K_S = 1399.2 \text{ MPa}$	$A_V = 619.3 \text{ MPa}$
$n_H = 0.089$	$n_L = 0.161$	$n_S = 0.0895$	$B_V = 1311 \text{ MPa}$
	$\sigma_0 = 500 \text{ MPa}$	$\varepsilon_0 = 9.35 \cdot 10^{-6}$	$n_V = 53.331$

Furthermore, we can examine correlations of some of the previously mentioned parameters.

The value of e_u (the engineering uniform strain) was computed using equation (2):

$$e_u = \frac{\Delta L_{Fmax}}{L_0} = \frac{1.6706}{30} = 0.0557 \quad (32)$$

from which the true engineering strain can be computed using equation (12):

$$\varepsilon_u = \ln(1 + e_u) = \ln(1 + 0.0557) = 0.0542 \quad (33)$$

As mentioned, this value can correlate in some cases with the exponent of Hollomon's relationship n_H (chapter 3.2). The difference of these numbers is:

$$d_H = 100 \left| \frac{n_H - \varepsilon_u}{\varepsilon_u} \right| = 100 \left| \frac{0.089 - 0.0542}{0.0542} \right| = 64.19 \% \quad (34)$$

Thus, we can say, that in the case of investigated 18CrNiMo7-6, the identified parameter n_H does not represent uniform strain ε_u , because the values vary by 64.19 %.

We can also examine the difference of 0.1% proof stress and the coefficient A_V in Voce's relationship (chapter 3.5). The 0.1% proof stress was identified from stress-strain curve - $s_{p0.1} = 614.9 MPa$, which gives a good correlation with value of $A_V = 619.25 MPa$. The difference between these two numbers is only

$$d_V = 100 \left| \frac{s_{p0.1} - A_V}{s_{p0.1}} \right| = 100 \left| \frac{614.9 - 619.25}{614.9} \right| = 0.71 \% \quad (35)$$

6. Summary and conclusion

This thesis can be divided into two major parts.

In the first part (chapters 2 and 3), the research study was carried out, including descriptions of the tensile test, differences between engineering and true stress and strain and their relationships, an analytical correction method (MLR) for obtaining average equivalent stress–strain curve beyond the necking initiation, the summary of elasto-plastic material models and the properties of four chosen non-linear relationships.

The second part (chapters 4 and 5) applied previous research to the experimental case of the tensile test of 18CrNiMo7-6 steel. The APDL macro was developed and piece-wise linear flow curve was identified and calibrated on the basis of force response from the simulation and experiment. The force response from the simulation did not differ more than 1.5 % from the experiment in the region of plastic instability. Then, the user interface was designed for fitting the four chosen non-linear relationships, mentioned above. The best fit was found using Swift's relationship, giving the lowest root-mean square error and good correlation found between identified Voce's coefficient A_V and experimentally identified proof stress $s_{p0.1}$. Identified parameters of Hollomon's relationship can be furthermore used for solving e.g. flow stress magnitude for certain true strain value in forming processes.

There is a potential in research in the flow curve identification procedure, especially in its optimization and automatization. It is difficult to make the process automatized, since the material properties vary dramatically in the fields of mechanical engineering. Especially challenging are descriptions of yield-point elongations. New methods of identification (soft computing – neural networks, sequential simulations [4]) were proposed, yet the versatility is still limited, and methods can be investigated and optimized further.

7. References

- [1] ASM INTERNATIONAL.: *ASM handbook. 10th ed., Vol. 8, Mechanical Testing and Evaluation*. Materials Park, OH: ASM International, ISBN-10: 0871703890, 2000.
- [2] JENÍK, I.: *Identifikace parametrů elasto-plastických modelů materiálu z experimentálních dat*. Brno: Brno University of Technology, Faculty of mechanical engineering, pp. 87. Supervisor Ing. Petr Kubík, 2015.
- [3] PTÁČEK, L.: *Nauka o materiálu I*. Brno: CERM, ISBN: 80-7204-193-2, 2001.
- [4] JENÍK, I., KUBÍK, P., ŠEBEK, F., HŮLKA, J., PETRUŠKA, J.: *Sequential simulation and neural network in the stress–strain curve identification over the large strains using tensile test*. Archive of Applied Mechanics, vol. 87, no. 6, pp. 1077-1093, DOI:10.1007/s00419-017-1234-0, 2017.
- [5] REES, D. W. A.: *Basic engineering plasticity: An introduction with engineering and manufacturing applications*. Boston, MA: Elsevier, ISBN-13: 978-0750680257, 2006.
- [6] BOŘKOVEC, J.: *Výpočtová simulace procesu dělení materiálu*. Brno: Brno University of Technology, Faculty of mechanical engineering, pp. 100. Supervisor prof. Ing. Jindřich Petruška, CSc., 2008
- [7] MIRONE, G.: *A new model for the elastoplastic characterization and the stress-strain determination on the necking section of a tensile specimen*. International Journal of Solids and Structures, vol. 41, no. 13, pp. 3545-3564, DOI:10.1016/j.ijsolstr.2004.02.011, 2004.
- [8] KLEEMOLA, H. J., NIEMINEN, M. A.: *On the strain-hardening parameters of metals*. Metallurgical Transactions, vol. 5, no. 8, pp. 1863-1866, DOI:10.1007/BF02644152, 1974.
- [9] HOLLomon, H. J.: *Tensile Deformation*. Metals Technology, pp.268-290, 1945.
- [10] SAMUEL, K. G.: *Limitations of Hollomon and Ludwigson stress–strain relations in assessing the strain hardening parameters*. Journal of Physics D: Applied Physics, vol. 39, pp. 203-212. DOI: 10.1088/0022-3727/39/1/030. ISSN 0022-3727, 2006.
- [11] SWIFT, H. W.: *Plastic instability under plane stress*. Journal of the Mechanics and Physics of Solids, vol. 1, no. 1, pp. 1-18, DOI:10.1016/0022-5096(52)90002-1, 1952.
- [12] VOCE, E.: *The relationship between stress and strain for homogeneous deformation*. Journal of Institute of Metals, vol. 74, pp.537-62, 1948.

8. Lists

8.1. List of abbreviations

APDL	ANSYS Parametric Design Language
ASTM	American Standard for Testing and Materials
DIN	„ <i>Deutsches Institut für Normung</i> “ – German Institute for Standardization
EN	European Standards
FEM	Finite Element Method
MLR	Mirone-La Rosa correction method

8.2. List of variables

A	instantaneous cross-sectional area of specimen	$[\text{mm}^2]$
A_0	undeformed cross-sectional area of specimen	$[\text{mm}^2]$
A_f	final cross-sectional area of fractured specimen	$[\text{mm}^2]$
A_V	initial (or threshold) stress in Voce's relationship	$[\text{MPa}]$
B_V	final constant stress in Voce's relationship	$[\text{MPa}]$
d	percental difference of two numbers	$[\%]$
d_0	original diameter	$[\text{mm}]$
d_f	diameter at fracture	$[\text{mm}]$
e	engineering (or average linear) strain	$[-]$
E	Young's modulus	$[\text{MPa}]$
e_f	elongation (or engineering strain at fracture)	$[\%]$
Er	least square error	$[-]$
e_u	engineering uniform strain	$[-]$
e_x	axial engineering strain (direction in axis x)	$[-]$
e_y	transverse engineering strain (direction in axis y)	$[-]$
e_z	transverse engineering strain (direction in axis z)	$[-]$
F	applied load	$[\text{N}]$
F_{exp}	force measured in experimental tensile test	$[\text{N}]$
F_{max}	maximum force measured in tensile test	$[\text{N}]$

F_y	reaction force from the tensile test simulation	[N]
K_H	strain hardening coefficient (or strength coefficient) in Hollomon's relationship	[MPa]
K_L	strength coefficient in Ludwik's relationship	[MPa]
K_S	strength coefficient in Swift's relationship	[MPa]
K_V	dimensionless constant in Voce's relationship	[–]
L	instantaneous deformed length of specimen	[mm]
L_0	gauge (or original undeformed) length of specimen	[mm]
L_{0ext}	distance between extensometer's clips	[mm]
L_f	final length of a fractured specimen	[mm]
MLR_ε	Mirone's correction coefficient for strain	[–]
MLR_σ	Mirone's correction coefficient for stress	[–]
n_H	Hollomon's strain hardening exponent	[–]
n_L	exponent in Ludwik's relationship	[–]
nl	number of loadsteps	[–]
n_S	exponent in Swift's relationship	[–]
n_V	exponent in Voce's relationship	[–]
pt	number of points of flow curve	[–]
q	area reduction	[%]
s	engineering stress	[MPa]
s_e	yield point	[MPa]
s_{eH}	upper yield point	[MPa]
s_{eL}	lower yield point	[MPa]
s_m	ultimate tensile strength	[MPa]
s_{pxx}	proof stress of xx % of strain	[MPa]
UX	boundary condition; fixed displacement in the global direction of x	[mm]
UY	boundary condition; fixed displacement in the global direction of y	[mm]
UY_{ext}	boundary condition; displacement in the global direction of y	[mm]
ΔL	increment of elongation	[mm]
ΔL_{Fmax}	increment of elongation on maximum load	[mm]
ε	true (or logarithmic) strain	[–]
ε_0	constant true strain value in Swift's relationship	[–]

$\varepsilon_{eq,avg}$	corrected average equivalent strain	[–]
$\varepsilon_{eq,f}$	equivalent fracture strain	[–]
ε_N	true strain at necking initiation	[–]
ε_{pl}	true (or equivalent) plastic strain	[–]
ε_u	true uniform strain	[–]
ν	Poisson's ratio	[–]
σ	true (or equivalent) stress	[MPa]
σ_0	yield point stress value in Ludwik's equation	[MPa]
$\sigma_{eq,avg}$	corrected average equivalent stress	[MPa]
σ_{fit}	equivalent stress value of fitted curve	[MPa]
$\sigma_{flow\ curve}$	equivalent stress value of flow curve	[MPa]
σ_N	true stress at necking initiation	[MPa]
σ_x	true axial stress component	[MPa]
σ_y	true radial stress component	[MPa]
σ_z	true circumferential stress component	[MPa]

8.3. List of attachments

<i>comparison.m</i>	MATLAB script for loading and comparing reaction force difference between simulation and experiment. Simultaneously it plots current flow curve.
<i>experiment.dat</i>	an force-elongation output of experimental tensile test measurement of 18CrNiMo7-6 steel.
<i>feedback.dat</i>	an output of the FEM simulation – the load–elongation dependency
<i>fitting_GUI.fig</i>	graphical environment of the created user interface for fitting non-linear relationships, used by the created code
<i>fitting_GUI.m</i>	code of the created user interface for fitting non-linear relationships
<i>fl_eps.txt</i>	material input of flow curve – equivalent strain
<i>fl_sig.txt</i>	material input of flow curve – equivalent stress
<i>macro.mac</i>	APDL macro for FEM simulation of tensile test
<i>Main Document.pdf</i>	an electronic version of this document
<i>table.pdf</i>	table with percental difference between reaction force of simulation and experiment